

## CHAPTER 3: RESULTS AND DISCUSSION

### 3.1 Syntheses of the compounds studied

Reactions of 2-chloropyrazine (**11**) with a series of piperidines, anilines and phenols were studied as shown in Figure 3.1.

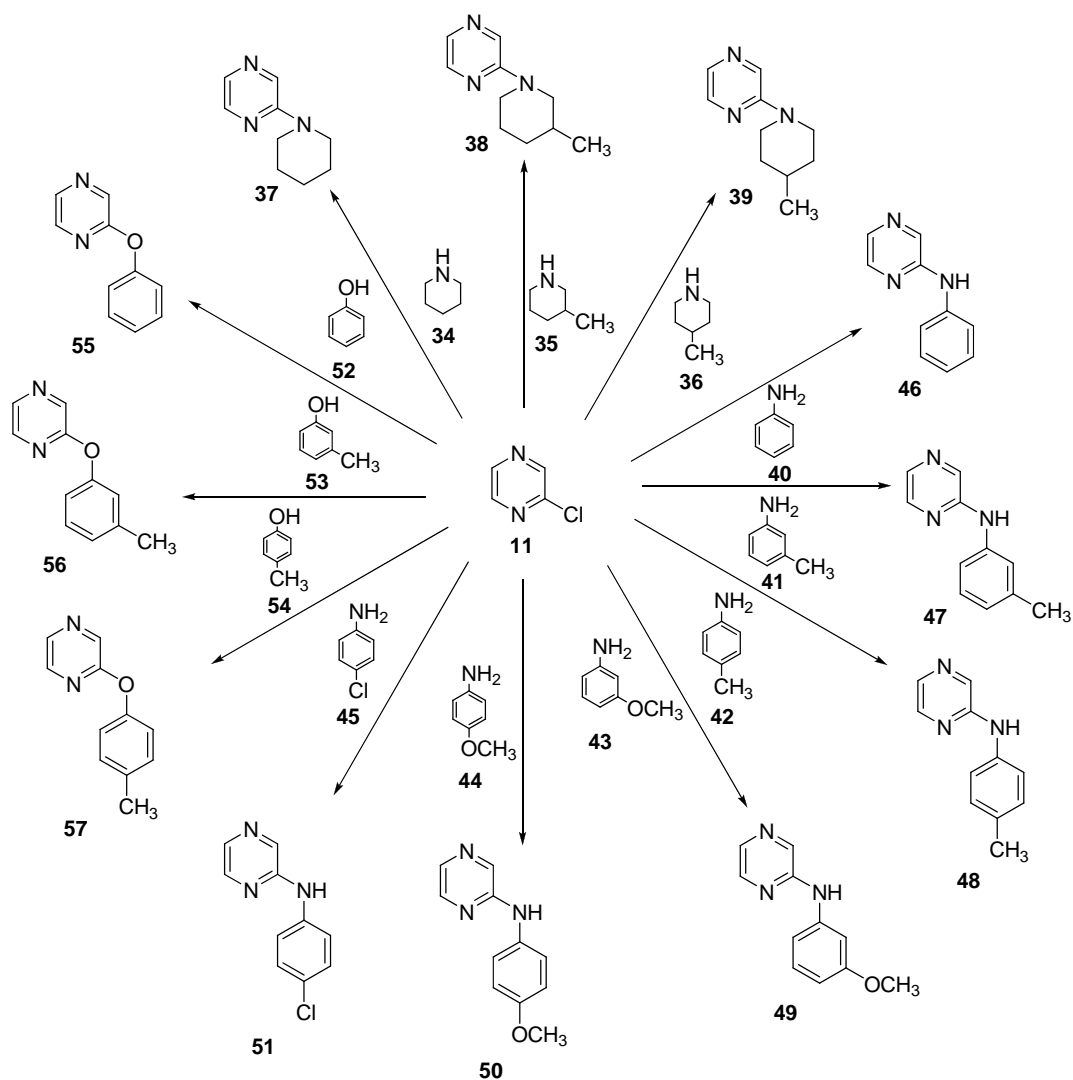
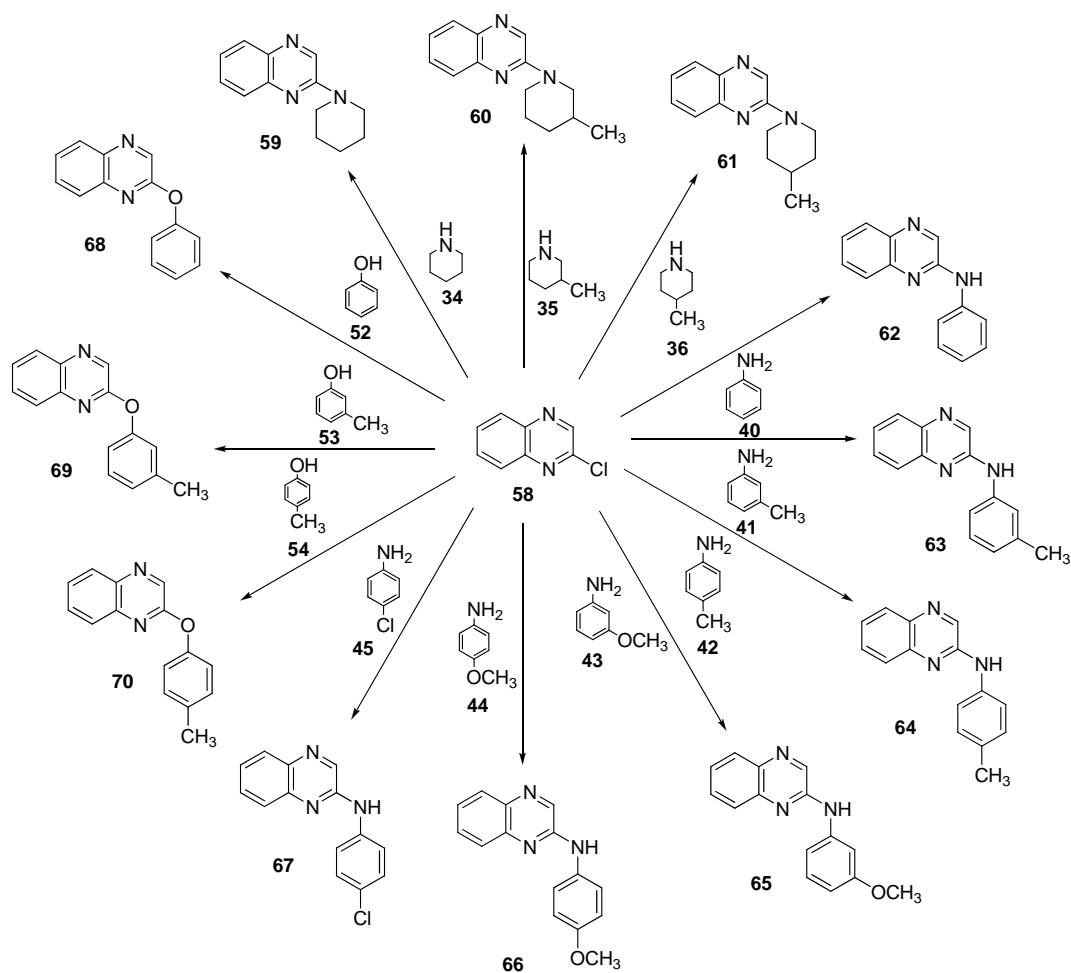


Figure 3.1: 2-Substituted pyrazines prepared

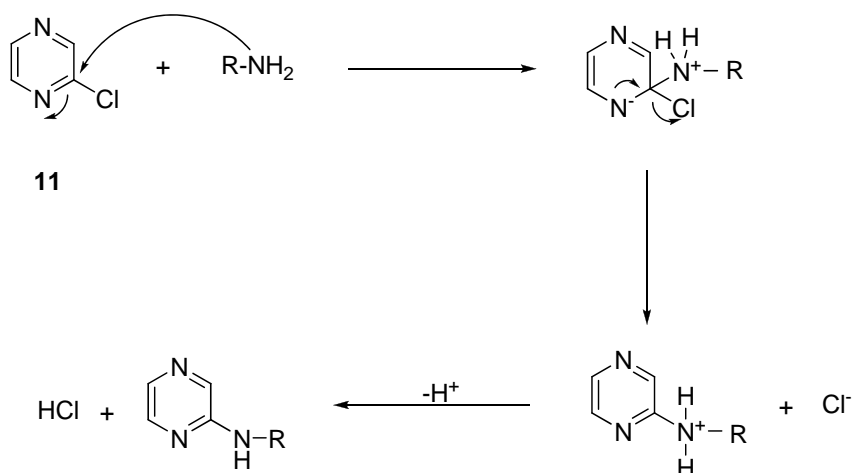
Reactions of 2-chloroquinoxaline (**58**) with a series of piperidines, anilines and phenols were prepared and as shown in Figure 3.2.



**Figure 3.2: 2-Substituted quinoxalines prepared**

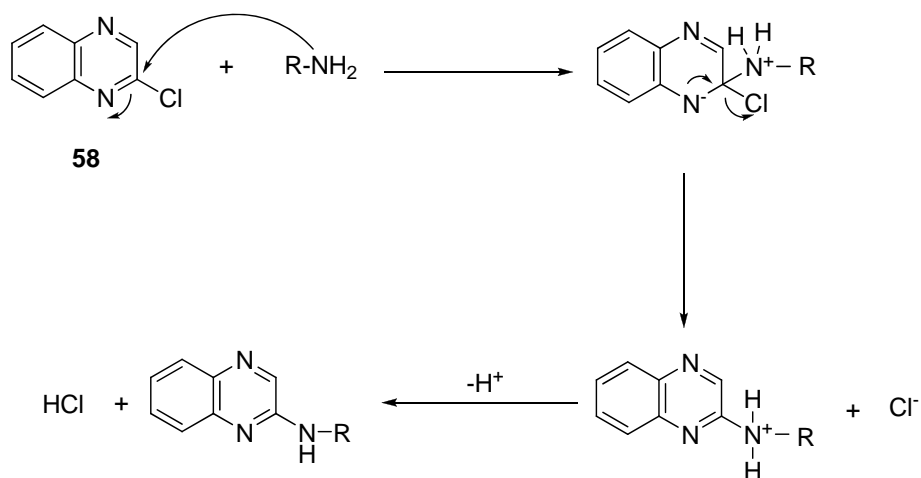
The structures of 2-substituted pyrazines and 2-substituted quinoxalines were confirmed by IR,  $^1\text{H}$  NMR,  $^{13}\text{C}$  NMR and GC-mass spectra. All the detailed spectra are attached in appendix section.

In general, the 2-position of pyrazine ring is activated towards nucleophilic attack. This is due to the presence of the adjacent electron withdrawing nitrogen atom. The reaction occurs at the second position of pyrazine with a nucleophile is as shown in the Scheme 3.1:



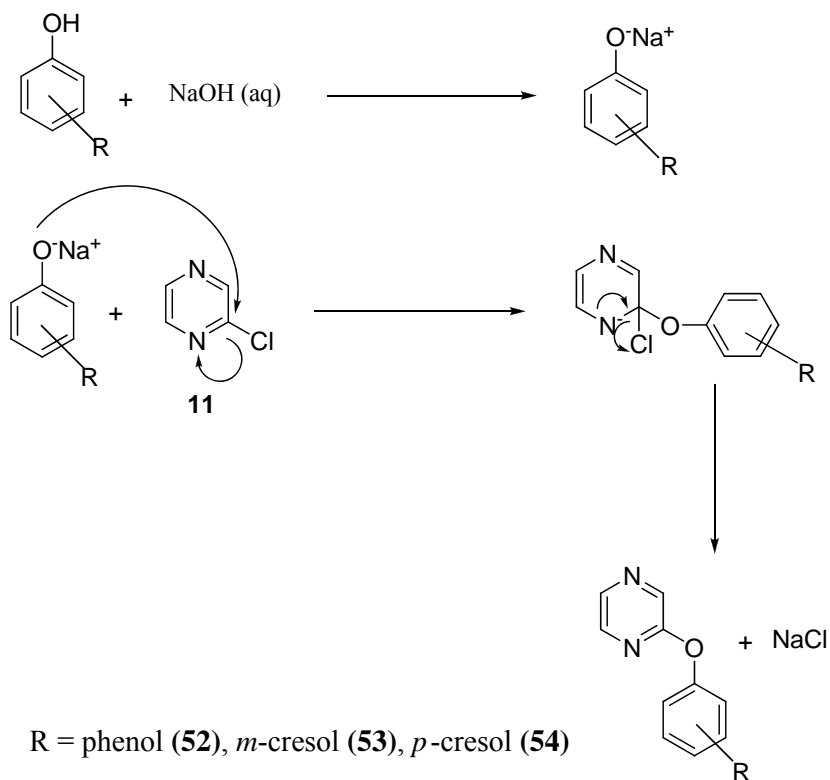
**Scheme 3.1: Nucleophilic substitution at position 2 of pyrazine system**

Similarly with the 2-position of quinoxaline ring, the ring is activated towards nucleophilic attack. The reaction occurs is as shown in the Scheme 3.2:



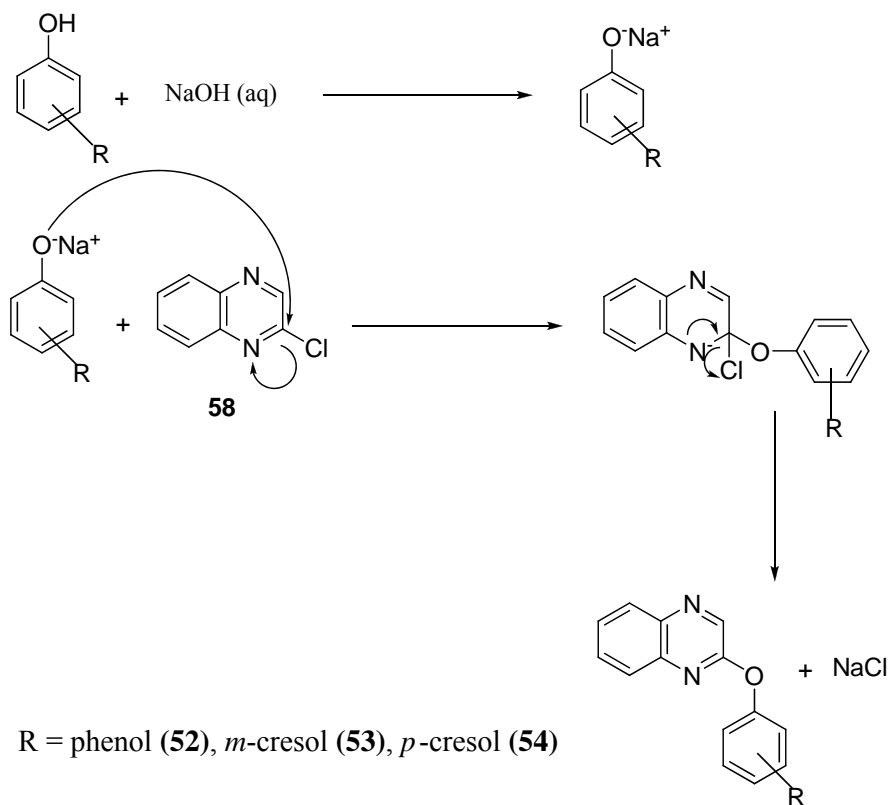
**Scheme 3.2: Nucleophilic substitution at position 2 of quinoxaline system**

Reactions of 2-chloropyrazine (**11**) with phenol (**52**), *m*-cresol (**53**) and *p*-cresol (**54**) were carried out using the classical Williamson ether synthesis.<sup>111</sup> This method of preparing unsymmetrical ethers is still thought of as one of the best methods for preparing ethers. The reaction of 2-chloropyrazine (**11**) with phenols is as shown in Scheme 3.3.



**Scheme 3.3: Formation of 2-phenoxy pyrazines**

Similarly with the 2-chloroquinoxaline (**58**), the reactions were carried out with phenol (**52**), *m*-cresol (**53**) and *p*-cresol (**54**). The reaction of 2-chloroquinoxaline (**58**) with phenols is as shown in Scheme 3.4.



**Scheme 3.4: Formation of 2-phenoxyquinoxalines**

## 3.2 Syntheses of pyrazine derivatives

### 3.2.1 Reactions of 2-chloropyrazine with piperidine and its derivatives

Reactions of 2-chloropyrazine (**11**) with piperidine (**34**), 3-methylpiperidine (**35**) and 4-methylpiperidine (**36**) were studied and as shown in Figure 3.3.

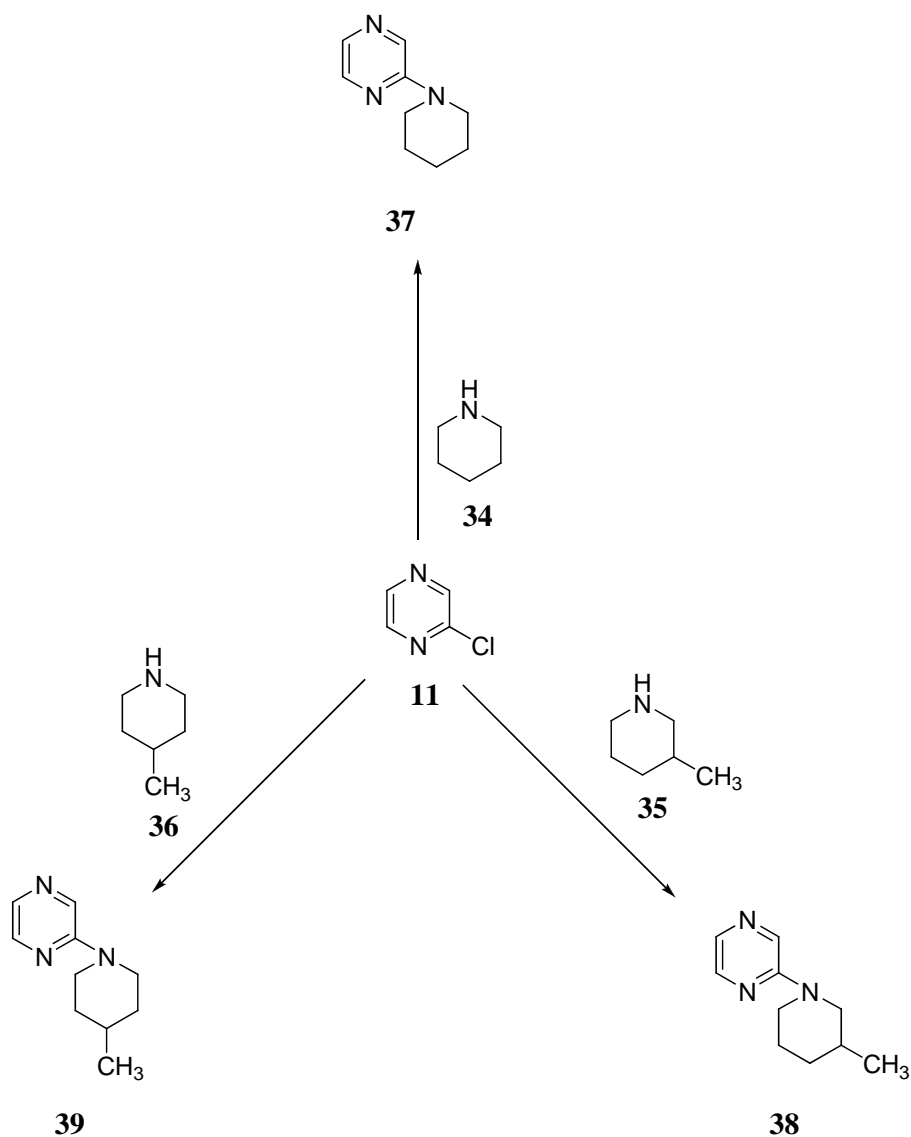
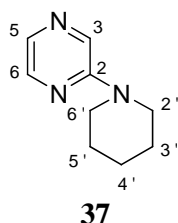


Figure 3.3: Reactions of 2-chloropyrazine with piperidine and its derivatives

2-*N*-piperidinopyrazine (**37**) was obtained when 2-chloropyrazine (**11**) was added to a solution of piperidine (**34**) in ethanol. The mixture was heated under reflux for 2 hours. The product was obtained through partition with diethyl ether and water. Evaporation of ethanol gave a yellowish liquid which repeatedly washed with diethyl ether to yield the pure product of 76%. The detailed experimental procedure is given in Chapter 5.

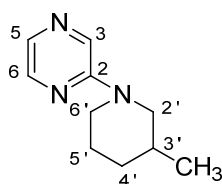
The infrared spectrum of (**37**) showed a weak absorption band at  $1672\text{ cm}^{-1}$  and a medium absorption band at  $1517\text{ cm}^{-1}$  which were due to C=N and C=C stretchings, respectively. A strong absorption band was also observed at  $2935\text{ cm}^{-1}$  and this was due to C-H stretching. The mass spectrum showed a  $[M^+]$  peak at  $m/z$  163 corresponding to the molecular formula  $C_9H_{13}N_3$ .



The  $^1\text{H}$  NMR spectrum showed a doublet with coupling constant of 1.4 Hz at  $\delta$  8.05 which was due to H-3. H-5 was observed as doublet of doublets at  $\delta$  7.96 with coupling constant of 2.6 Hz and 1.4 Hz. A doublet peak was observed at  $\delta$  7.69 with coupling constant of 2.6 Hz which was assigned to H-6. Two broad singlets were observed in the aliphatic region of  $\delta$  3.49 and  $\delta$  1.55, which were due to the H-2', H-6' and H-3', H-4', H-5' respectively.

The  $^{13}\text{C}$  NMR spectrum indicated the presence of 9 carbon atoms. The carbons of pyrazine ring were observed at  $\delta$  155.0,  $\delta$  141.6,  $\delta$  131.7, and  $\delta$  130.9 which were assigned to C-2, C-3, C-5 and C-6 respectively. The signals at  $\delta$  45.4 -  $\delta$  24.4 in the high field region were attributable to the carbons of the piperidine ring. The full proton and carbon assignments were summarized in the Chapter 5.

The reaction of 2-chloropyrazine (**11**) with 3-methylpiperidine (**35**) produced 2-*N*-(3-methyl)piperidinopyrazine (**38**). The reaction was refluxed for 5 hours without any solvent used to give a 34% yield of the product. The infrared spectrum of (**38**) showed similar absorptions to that of 2-*N*-piperidinopyrazine (**37**). Peaks at  $1673\text{ cm}^{-1}$  and  $1517\text{ cm}^{-1}$  were recorded which were due to the stretching frequencies of C=N and C=C bonds. Mass spectrum displayed the  $[\text{M}^+]$  peak at  $m/z$ : 177.25 which is in well agreement with the molecular formula  $\text{C}_{10}\text{H}_{15}\text{N}_3$ .

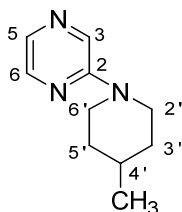


**38**

The  $^1\text{H}$  NMR spectrum of (**38**) showed similar absorption peaks as compound (**37**) in the regions of  $\delta$  8.04 -  $\delta$  7.66 which were due to H-3, H-5 and H-6. A doublet peak was observed at  $\delta$  4.10 which was assigned to H-6'. In addition, H-2' were observed as triplet of doublets (td) and triplet at  $\delta$  2.73 and  $\delta$  2.41 with coupling constant of 12.6 Hz, 2.9 Hz and 10.9 Hz. H-5' and H-4' were recorded as multiplets at  $\delta$  1.42, whereas H-3' was observed at  $\delta$  1.03. A doublet peak with coupling constant of 6.5 Hz was recorded at  $\delta$  0.86 indicated the presence of a methyl group.

The  $^{13}\text{C}$  NMR spectrum showed a total of 10 carbons where four of them were resonated in the downfield aromatic region of pyrazine ring between  $\delta$  155.0 –  $\delta$  131.1. Five signals in the up-field region of  $\delta$  52.2 -  $\delta$  24.8 were assigned to carbons on piperidine ring, while the methyl carbon resonated at  $\delta$  19.3.

A 77% yield of pure 2-*N*-(4-methyl)piperidinopyrazine (**39**) was obtained when 2-chloropyrazine was allowed to react with 4-methylpiperidine. The IR spectrum showed absorption bands at  $1673\text{ cm}^{-1}$ ,  $1518\text{ cm}^{-1}$  and  $2924\text{ cm}^{-1}$  indicating the presence of C=N, C=C and due to C-H stretchings respectively. The mass spectrum showed a molecular ion at  $m/z$  177, which corresponded to the molecular formula  $\text{C}_{10}\text{H}_{15}\text{N}_3$ .



**39**

The  $^1\text{H}$  NMR spectrum of (**39**) showed a doublet at  $\delta$  8.08 with coupling constant of 1.4 Hz which was due to the H-3. H-5 was observed as doublet of doublets (dd) at  $\delta$  7.98 with coupling constant of 2.6 Hz and 1.4 Hz. Doublets were recorded at  $\delta$  7.69 and  $\delta$  4.22 which were assigned to H-6 and H-2'. Each doublet having coupling constant of 2.6 Hz and 12 Hz. In addition, H-6' was observed as triplet of doublets (td) at  $\delta$  2.79 with coupling constant of 12.6 Hz and 2.4 Hz. A doublet peak at  $\delta$  2.60 with coupling constant of 12 Hz was assigned to H-3'. Two multiplet peaks recorded at  $\delta$  1.54 and  $\delta$  0.99 were assigned to the H-4' and H-5' while hydrogen of the methyl group signal was observed as a doublet at  $\delta$  0.85.

The  $^{13}\text{C}$  NMR spectrum showed a total of 10 carbon peaks which consist of one methyl carbon, five methylene carbons, three methine carbons and one quaternary carbon. The most downfield signals at  $\delta$  155.1-  $\delta$  131.2 were assigned to C-2, C-3, C-5 and C-6 of the pyrazine ring. Three absorption peaks were observed in aliphatic region which were due to the carbons on the piperidine ring. In the up-field region, the absorption peak at  $\delta$  21.9 was observed which was due to the carbon resonance of the methyl group.

### 3.2.2 Reactions of 2-chloropyrazine with aniline and its derivatives

Reaction of 2-chloropyrazine (**11**) with aniline (**40**), *m*-toluidine (**41**), *p*-toluidine (**42**), *m*-anisidine (**43**), *p*-anisidine (**44**) and *p*-chloroaniline (**45**) were studied. Figure 3.4 shows a diagrammatic representation of various reactions.

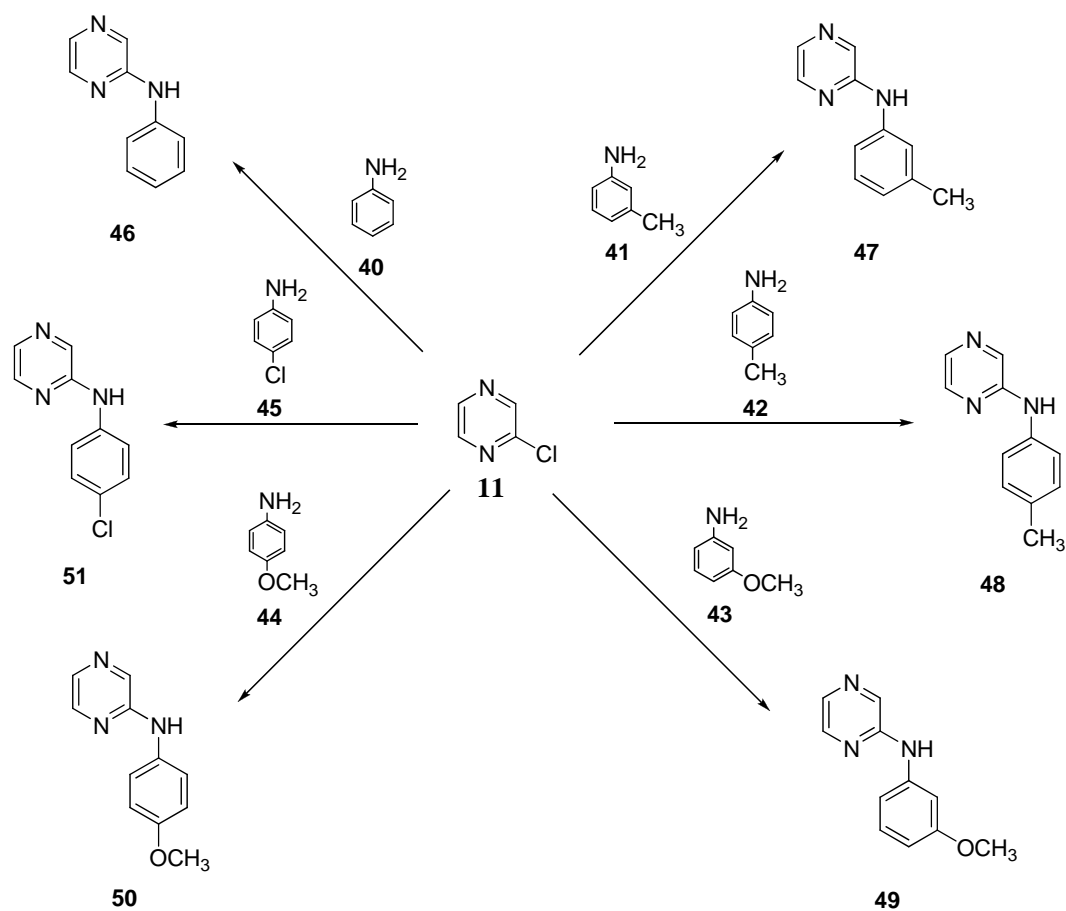
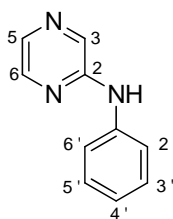


Figure 3.4: Reactions of 2-chloropyrazine with aniline and its derivatives

The reaction of 2-chloropyrazine (**11**) with aniline (**40**) gave 69% yield when the mixture of two compounds were heated under reflux at 120°C-140°C for 3 hours. Isolation of the product (**46**) was accomplished through extraction with diethyl ether followed by successive washing with water. Recrystallisation from chloroform gave colourless crystals of (**46**).

The infrared spectrum of compound (**46**) showed weak absorption bands at 1624 cm<sup>-1</sup> and 1585 cm<sup>-1</sup> which were due to C=N stretching and N-H bending. A weak band was observed at 3281cm<sup>-1</sup> which was due to the N-H stretching of the secondary amine. Medium and strong absorption bands which were recorded at 697 cm<sup>-1</sup> and 755 cm<sup>-1</sup> indicating a monosubstituted benzene ring. The GC-mass spectrum of (**46**) showed a molecular ion at *m/z* 171.



**46**

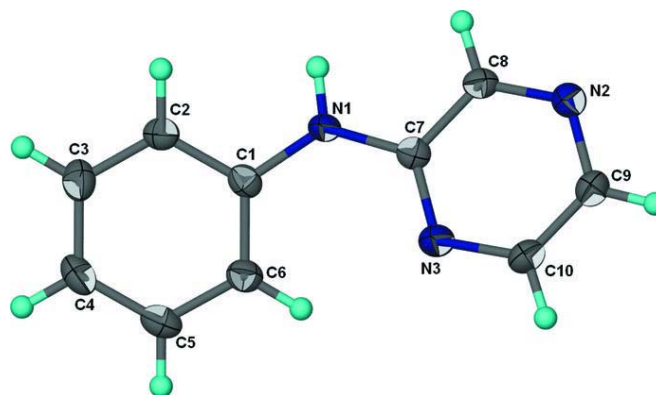
The <sup>1</sup>H NMR spectrum of (**46**) showed similar absorption peaks as compound (**39**) in the regions of δ 8.25 - δ7.97, which were due to H-3, H-5 and H-6 of pyrazine ring. A doublet at δ 7.42 with *J* value of 7.8 Hz and a triplet at δ 7.34 with *J* value of 7.3 Hz were attributed to H-2', H-6' and H-3', H-5' respectively. A triplet which observed at δ 7.09 with coupling constant of 7.3 Hz was assigned to H-4' of the aniline ring. A singlet observed at δ 6.74 was assigned to N-H peak.

The  $^{13}\text{C}$  NMR spectrum of **(46)** showed relatively low intensity absorption peaks at  $\delta$  152.3 and  $\delta$  139.1 which were due to quaternary carbon resonances of C-2 and C-1' respectively. Three medium peaks at  $\delta$  141.9,  $\delta$  134.9 and  $\delta$  132.9 were recorded which believed from the carbon resonance of C-3, C-5, and C-6 of the pyrazine ring, whilst C-4' of the aniline ring was recorded at  $\delta$  123.6. In addition, two relatively high intensity peaks at  $\delta$  129.4 and  $\delta$  120.3 were recorded due to the two carbon resonances of C-2', C-6' and C-3', C-5' of the aniline ring.

Recrystallisation of 2-*N*-anilinopyrazine **(46)** in ethanol gave colourless crystals which was analysed by X-ray diffraction method. The crystal **(46)** has a monoclinic system,  $P2_1/c$ . The two aromatic rings in compound **(46)** as shown in Figure 3.5, are inclined at  $15.2 (1)^\circ$  to each other. This opens up the angle at the amino nitrogen atom to  $130.4 (1)^\circ$ . The amino nitrogen forms a hydrogen bond to the 4-nitrogen atom of an adjacent molecule to furnish a chain motif.<sup>112</sup> The crystals system and refinement data are shown in Table 3.1. Figure 3.5 shows the thermal ellipsoid of compound **(46)** at the 70% probability level, hydrogen atoms were drawn as spheres of arbitrary radius.

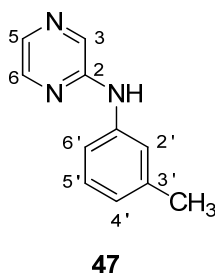
**Table 3.1: Crystal data and structure refinement for 2-*N*-anilinopyrazine (46)**

Identification code	<i>N</i> -(Pyrazin-2-yl)aniline
Empirical formula	C <sub>10</sub> H <sub>9</sub> N <sub>3</sub>
Formula weight	171.20
Colour	colourless
Crystal system, space group	Monoclinic, P-21/c
Unit cell dimensions	$a = 11.0644 (3) \text{ \AA}$ $b = 7.8423 (3) \text{ \AA}$ $c = 10.8907 (3) \text{ \AA}$ $\beta = 116.439 (2)^\circ$
$V (\text{\AA}^3)$	846.15 (5)
$Z$	4
$\rho_{\text{calc}}$ (Mg m <sup>-3</sup> )	1.344
Absorption coefficient (mm <sup>-1</sup> )	0.09
$F(000)$	360
Crystal size (mm)	0.20 x 0.10 x 0.05
$\theta_{\text{max}}$	27.5°
$\leq h \leq$	-14 to 14
$\leq k \leq$	-10 to 10
$\leq l \leq$	-14 to 14
Reflections collected / unique	1934 / 1463
$R_{\text{int}}$	0.033
Completeness to theta	3.3 – 26.4
Data / restraints / parameters	1934 / 1 / 122
Goodness-of-fit on $F^2$	0.101
Final $R$ indices [ $I > 2\sigma(I)$ ]	0.041

**Figure 3.5: Ortep diagram of 2-*N*-anilinopyrazine (46)**

Treatment of 2-chloropyrazine (**11**) with 3-methylaniline (**41**) in 1:1 equivalent gave 60% yield of pure product, 2-*N*-(*m*-methyl)anilinopyrazine (**47**). In the first attempt, the reaction was carried out in ethanol as solvent. The percentage yield obtained was 26%. Better percentage yield was obtained when the reaction was carried out in the absence of ethanol. With the presence of solvent, the protonation of the solvent may be occurred towards the reaction mixture.

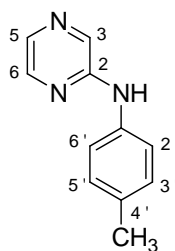
Compound (**47**) showed two absorption bands of medium intensity in an infrared spectrum at  $3298\text{ cm}^{-1}$  and  $1583\text{ cm}^{-1}$  which were due to N-H stretching and N-H bending. Similar absorption bands were observed as in compound (**46**) indicating the presence of C=N and aromatic C=C stretches except the addition of two bands at  $778\text{ cm}^{-1}$  and  $826\text{ cm}^{-1}$  which were the characteristic of *meta* disubstituted benzene ring. The mass spectrum showed a molecular ion at  $m/z$  185, which corresponds with the molecular formula  $\text{C}_{11}\text{H}_{11}\text{N}_3$ .



The  $^1\text{H}$  NMR spectrum of (**47**) showed a singlet at  $\delta$  8.17 which was due to the H-3. Signal at  $\delta$  8.02 was recorded as doublet of doublets with a coupling constant of 2.6 Hz and 1.4 Hz which were assigned to H-5. A doublet was observed at  $\delta$  7.88 with coupling constant of 2.6 Hz were assigned to H-6. Multiplet were observed at  $\delta$  7.13 corresponding to H-6', H-2', H-5'. A doublet peak recorded at  $\delta$  6.84 with  $J$  value of 8 Hz was due to the H-4'. A broad singlet observed at  $\delta$  6.60 was assigned to N-H peak. Meanwhile, the presence of protons of the methyl group was indicated by the observation of a singlet at  $\delta$  2.28.

The  $^{13}\text{C}$  NMR spectrum gave a total of 11 separate carbon resonances comprising 1 methyl carbon, 7 methine carbons and 3 quaternary carbons which are in agreement with the molecular formula of **(47)**. The relatively low intensity of quaternary carbons at  $\delta$  152.4 was assigned to C-2 of the pyrazine ring, while signals at  $\delta$  139.3 and  $\delta$  139.0 were assigned to C-1' and C-3' of the 3-methylaniline ring. The signals at  $\delta$  134.7 and  $\delta$  132.8 were attributable to C-5 and C-6 of the pyrazine ring. The signals at  $\delta$  117.5 -  $\delta$  129.2 were assigned to C-4', C-5', C-2' and C-6' of the 3-methylaniline ring. In addition, a peak observed at  $\delta$  21.5 in upfield region was due to  $\text{sp}^3$  carbon of methyl group of 3-methylaniline ring.

Reaction of 2-chloropyrazine **(11)** with 4-methylaniline **(42)** gave 19% yield of colourless crystals of compound **(48)**. The structure of 2-*N*-(*p*-methyl)anilinopyrazine **(48)** was confirmed by spectroscopic methods and the crystal structure was confirmed by X-ray diffraction method. The IR spectrum of compound **(48)** showed very similar absorptions of compound **(46)** except that an additional strong absorption peak was observed at  $812\text{ cm}^{-1}$ , indicating the *para* disubstitution of a benzene ring. The mass spectrum displayed  $[\text{M}^+]$  peak at  $m/z$  185 which consistent with the molecular formula  $\text{C}_{11}\text{H}_{11}\text{N}_3$ .



**48**

The  $^1\text{H}$  NMR spectrum of (**48**) showed similar absorption peaks as compound (**47**) in the region of  $\delta$  8.19 -  $\delta$ 7.93 which were due to H-3, H-5, H-6 of pyrazine ring. Two symmetrical peaks of doublets indicating the para disubstituted position which were recorded at  $\delta$  7.26 and  $\delta$  7.16 with the coupling constant of 8 Hz. These peaks were due to H-2', H-6' and H-3', H-5' of the aniline ring. Singlets peaks were observed at  $\delta$  6.62 and  $\delta$  2.34 indicating the presence of N-H and methyl group respectively.

The  $^{13}\text{C}$  NMR spectrum of (**48**) indicated the presence of 11 carbon atoms. The C-2, C-3, C-5 and C-6 of pyrazine ring were observed at  $\delta$  152.6, 134.5, 133.6, and 132.5 respectively. The signals at  $\delta$  141.9 and  $\delta$  136.3 were assigned to the C-1' and C-4' of the aniline ring. The relatively higher intensity absorption peaks at  $\delta$  129.9 and  $\delta$  121.0 were believed to be arised from the overlapping of carbon resonances of C-2', C-6' and C-3', C-5' of the aniline ring. The peak at  $\delta$  20.8 in the upfield region is notable for the presence of methyl group.

The structure of compound (**48**) was determined by X-ray crystallography. The crystals are colourless and having a monoclinic system, C2/c. The two aromatic systems in the (**48**) are inclined by  $19.1 (1)^\circ$ , whilst the angle at the central amino N atom is  $130.3 (2)^\circ$ . The amino group forms a hydrogen bond to the pyrazine N-4 atom of an adjacent molecule, forming a chain motif.<sup>113</sup> The crystals system and refinement data are shown in Table 3.2. Figure 3.6 shows the thermal ellipsoid plot of  $\text{C}_{11}\text{H}_{11}\text{N}_3$  at the 70% probability level, hydrogen atoms were drawn as spheres of arbitrary radius.

The crystals system and refinement data are shown in Table 3.2

**Table 3.2: Crystal data and structure refinement for 2-*N*-(*p*-methyl)anilinopyrazine (48)**

Identification code	<i>N</i> -(Pyrazin-2-yl)-4-toluidine
Empirical formula	C <sub>11</sub> H <sub>11</sub> N <sub>3</sub>
Formula weight	185.23
Colour	colourless
Crystal system, space group	Monoclinic, C2/c
Unit cell dimensions	$a = 21.7179 (7) \text{ \AA}$ $b = 7.5323 (3) \text{ \AA}$ $c = 12.0073 (5) \text{ \AA}$ $\beta = 105.790 (3)^\circ$
$V (\text{\AA}^3)$	1890.1 (1)
$Z$	8
$\rho_{\text{calc}}$ (Mg m <sup>-3</sup> )	1.302
Absorption coefficient (mm <sup>-1</sup> )	0.08
$F(000)$	784
Crystal size (mm)	0.30 x 0.20 x 0.05
$\theta_{\text{max}}$	27.5°
$\leq h \leq$	-28 to 28
$\leq k \leq$	-9 to 9
$\leq l \leq$	-15 to 15
Reflections collected / unique	2165 / 1437
$R_{\text{int}}$	0.041
Completeness to theta	2.0 – 27.5
Data / parameters	2165 / 132
Goodness-of-fit on $F^2$	0.046
Final $R$ indices [ $I > 2\sigma(I)$ ]	0.135

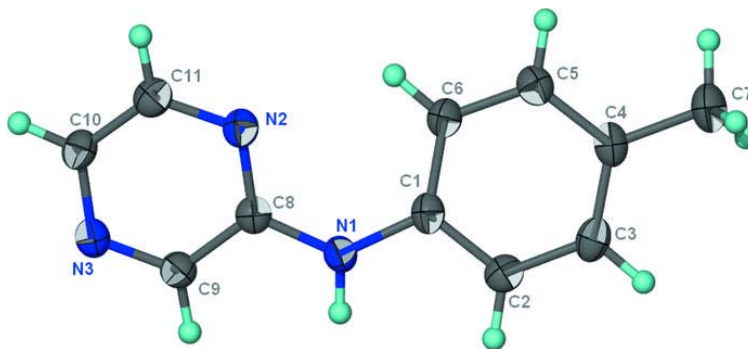
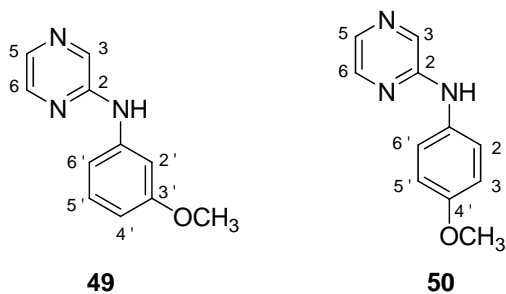


**Figure 3.6: Ortep diagram of 2-*N*-(*p*-methyl)anilinopyrazine (48)**

Reactions of 2-chloropyrazine (**11**) with *m*-anisidine (**43**) and *p*-anisidine (**44**) to form compounds (**49**) and (**50**) were carried out using similar method as recorded in Chapter 4. The infrared spectra display similar characteristic of the N-H and aromatic C=C stretching as well as N-H bending except for compound (**49**), the characteristic of *meta* disubstituted aromatic ring were observed as a strong band at 766 cm<sup>-1</sup> and medium band at 829 cm<sup>-1</sup>. Compound (**50**) on the other hand showed a strong band at 829 cm<sup>-1</sup> which was the characteristic of *para* disubstituted aromatic ring. The mass spectra of both compounds showed a molecular ion at *m/z* 201, which corresponds to the molecular formula C<sub>11</sub>H<sub>11</sub>N<sub>3</sub>O.



The <sup>1</sup>H NMR spectra of both compounds showed similar peaks in the region of δ 8.05 - δ 7.25 which were due to the protons on H-3, H-5 and H-6 of the pyrazine ring as previously discussed. A doublet of doublets at δ 7.21 with coupling constant of 8 Hz and 2.2 Hz of compound (**49**) was attributed to proton on H-6' of the aniline ring, whereas a singlet peak detected at δ 7.07 were assigned to H-2'. A doublet of doublets peaks were recorded at δ 6.93 and δ 6.61 with the coupling constant of 7.8 Hz and 4 Hz which were assigned to H-5', and H-4'.

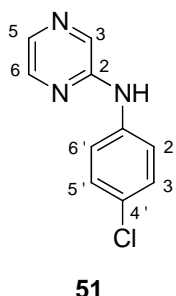
Compound (**50**), on the other hand showed a pair of doublets at  $\delta$  7.25 with  $J$  value of 8 Hz and  $\delta$  6.83 with  $J$  value of 8 Hz, were assigned to H-2', H-6' and H-3', H-5'. These symmetry peaks indicated the characteristic of *para* disubstituted position of compound (**50**). Two singlets which were recorded for both compounds at  $\delta$  6.60 and  $\delta$  3.70 were assigned to the N-H and methoxy group (-OCH<sub>3</sub>), respectively.

The <sup>13</sup>C NMR spectra of both compounds indicated the presence of 11 carbon atoms. In the most downfield region, three absorption peaks at  $\delta$  160.5,  $\delta$  152.1 and  $\delta$  140.2 were attributed to C-3', C-2 and C-3. Carbon resonances which were recorded at  $\delta$  141.8,  $\delta$  134.9,  $\delta$  133.1,  $\delta$  130.0,  $\delta$  112.4,  $\delta$  108.8 and  $\delta$  106.1 were assigned to C-1', C-5, C-6, C-6', C-2', C-5' and C-4' respectively. The most upfield signal at  $\delta$  55.3 was assigned to the OCH<sub>3</sub> group.

In the case of compound (**50**), a relatively low intensity absorption peaks at  $\delta$  156.7 was assigned to quaternary carbon C-4'. The other two quaternary carbons of C-2 and C-1' were recorded at  $\delta$  153.0 and  $\delta$  131.6 respectively. Three relatively medium intensity absorption peaks at  $\delta$  141.6,  $\delta$  134.0 and  $\delta$  132.2 were due to the carbon resonances of C-3, C-5 and C-6 on the pyrazine ring. Meanwhile, two high absorption peaks were recorded at  $\delta$  123.8 and  $\delta$  114.6 which arose from the C-2', C-6' and C-3', C-5' of the 4-methoxyaniline ring. In the upfield region, an absorption peak at  $\delta$  55.5 was due the carbon resonance of methoxy group.

2-*N*-(*p*-Chloro)anilinopyrazine (**51**) was obtained using similar method as in the preparation of compound (**49**) and (**50**). Instead of using *m*-anisidine and *p*-anisidine, *p*-chloroaniline was used. The pure product (**51**) was obtained after recrystallisation of the crude product using a minimum volume of chloroform. The structure of (**51**) was confirmed by IR, <sup>1</sup>H NMR, <sup>13</sup>C NMR, mass spectra and x-ray diffraction analysis.

The IR spectrum displayed absorption bands at 3246 cm<sup>-1</sup> and 1565 cm<sup>-1</sup>, which were due to the N-H stretch and N-H bending. A strong absorption band was observed at 821 cm<sup>-1</sup> which was assigned to *para* disubstituted benzene ring. The mass spectrum showed a [M<sup>+</sup>] peak at *m/z* 205 which represents the molecular formula C<sub>10</sub>H<sub>8</sub>N<sub>3</sub>Cl.



The <sup>1</sup>H NMR spectrum of (**51**) showed a doublet with *J* value of 1.4 Hz at δ 8.12 which was due to the H-3. Signal at δ 8.04 was recorded as doublet of doublets with coupling constant of 2.6 Hz and 1.4 Hz which was assigned to H-5. A doublet peak was observed at δ 7.93 with *J* value of 2.6 Hz which was due to the H-6. Doublets which were recorded at δ 7.43 and δ 7.23 with coupling constant of 6.8 Hz were corresponded to H-3', H-5' and H-2', H-6'. A broad singlet attributed to N-H was observed at δ 6.49.

The  $^{13}\text{C}$  NMR spectrum of (**51**) showed relatively low intensity absorption peaks at  $\delta$  151.8,  $\delta$  137.8 and  $\delta$  128.2 which were due to quaternary carbon resonance of C-2, C-4' and C-1' respectively. The signal assigned to C-4' was shifted downfield due to its position adjacent chlorine atom which more electronegative than bromine and iodine. Three relatively medium intensity absorption peaks at  $\delta$  141.7,  $\delta$  135.2 and  $\delta$  133.2 were due to the carbon resonances of C-3, C-5 and C-6 on the pyrazine ring. The high intensity absorption were observed at  $\delta$  129.3 was assigned to C-3' and C-5', whereas peak at  $\delta$  121.2 was assigned to C-2' and C-6'.

X-ray structure analysis showed that the structure of compound (**51**) are well shaped crystals which having a monoclinic system,  $P2_1/c$ . In the compound (**51**), the dihedral angle between the aromatic rings is  $43.0(1)^\circ$  and the bridging C—N—C angle is  $128.19(16)^\circ$ . The amino N atom of one molecule forms a hydrogen bond to the 1-N atom of an adjacent pyrazinyl ring, generating an inversion dimer.<sup>114</sup> The crystals system and refinement data are shown in Table 3.3. Figure 3.7 shows the thermal ellipsoid plot of  $\text{C}_{10}\text{H}_8\text{N}_3\text{Cl}$  at the 70% probability level, hydrogen atoms were drawn as spheres of arbitrary radius.

The crystals system and refinement data are shown in Table 3.3

**Table 3.3: Crystal data and structure refinement for 2-*N*-(*p*-chloro)anilino)pyrazine (51)**

Identification code	4-Chloro- <i>N</i> -(pyrazin-2-yl)aniline
Empirical formula	C <sub>10</sub> H <sub>8</sub> ClN <sub>3</sub>
Formula weight	205.64
Colour	yellow
Crystal system, space group	Monoclinic, P2 <sub>1</sub> /c
Unit cell dimensions	$a = 12.1257 (3) \text{ \AA}$ $b = 3.7944 (1) \text{ \AA}$ $c = 19.7242 (5) \text{ \AA}$ $\beta = 91.370 (2)^\circ$
$V (\text{\AA}^3)$	907.25 (4)
$Z$	4
$\rho_{\text{calc}}$ (Mg m <sup>-3</sup> )	1.506
Absorption coefficient (mm <sup>-1</sup> )	0.38
$F(000)$	424
Crystal size (mm)	0.25 x 0.05 x 0.01
$\theta_{\text{max}}$	28.1°
$\leq h \leq$	-15 to 15
$\leq k \leq$	-4 to 4
$\leq l \leq$	-25 to 24
Reflections collected / unique	2073 / 1633
$R_{\text{int}}$	0.033
Completeness to theta	1.7 – 27.5
Data / restraints / parameters	2073 / 1 / 131
Goodness-of-fit on $F^2$	0.037
Final $R$ indices [ $I > 2\sigma(I)$ ]	0.128

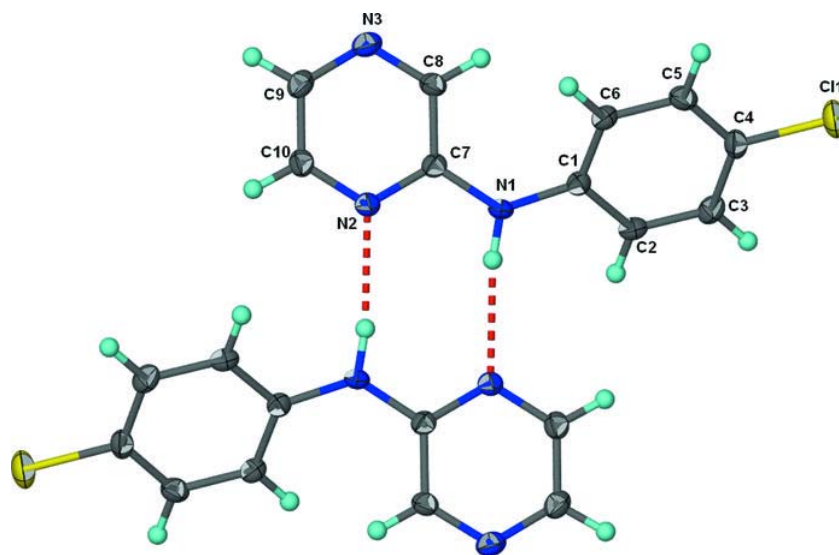


**Figure 3.7: Ortep diagram of 2-*N*-(*p*-chloro)anilino)pyrazine (51)**

### 3.2.3 Reaction of 2-chloropyrazine with phenol and cresols

Reaction of 2-chloropyrazine (**11**) with phenol (**52**), *m*-cresol (**53**) and *p*-cresol (**54**) were studied and as shown in Figure 3.8.

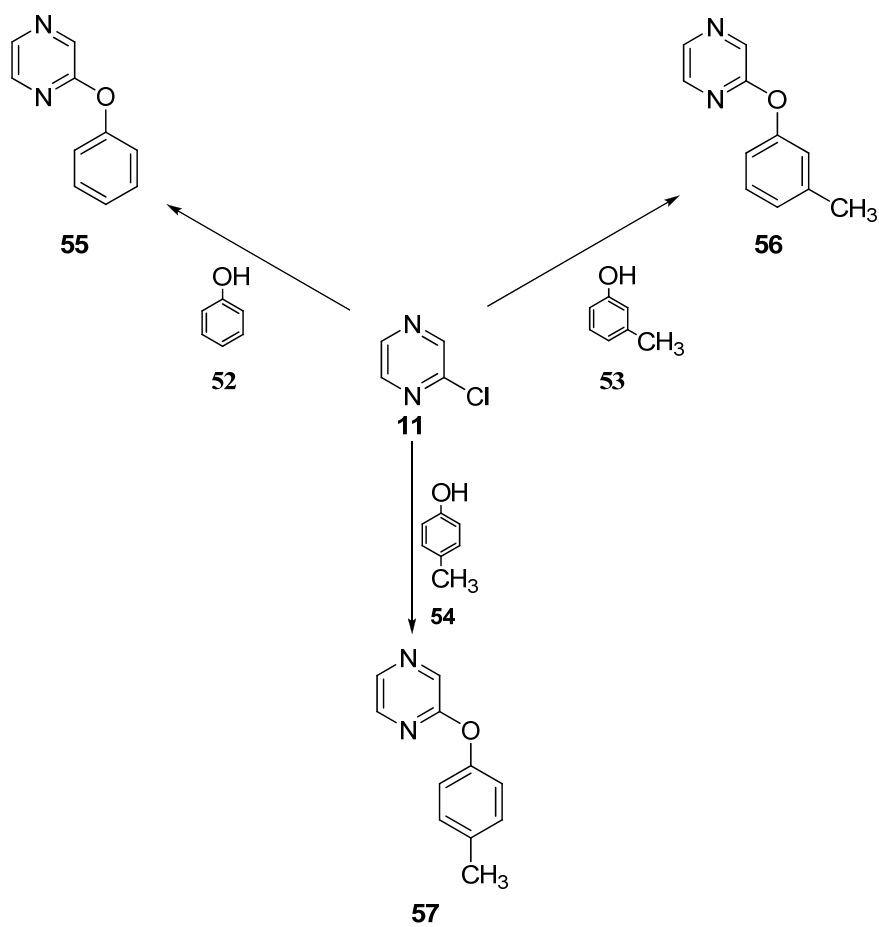
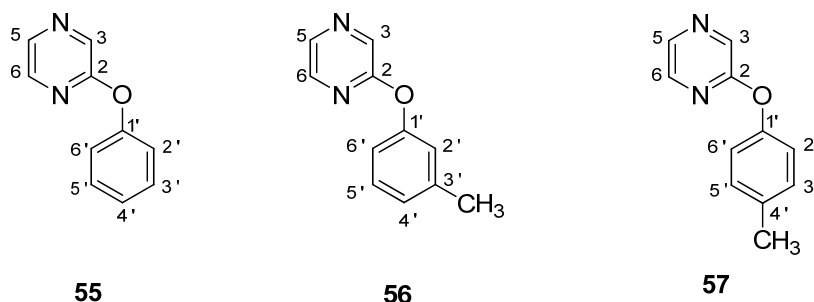


Figure 3.8: Reactions of 2-chloropyrazine with phenol and cresols

2-Phenoxy pyrazine (**55**) was obtained when phenol was added with sodium hydroxide pellet in minimum volume of water and heated under reflux for 5 hours. The same procedure was used for the preparation of 2-(*m*-methyl)phenoxy pyrazine (**56**) and 2-(*p*-methyl)phenoxy pyrazine (**57**). All pure products were obtained after recrystallisation.

Compounds (**55**), (**56**), and (**57**) showed medium intensity bands at  $1578\text{ cm}^{-1}$  to  $1612\text{ cm}^{-1}$  in IR spectra, which were due to the presence of C=N of the pyrazine ring and aromatic C=C stretching. High intensity bands observed at  $1284\text{ cm}^{-1}$  and  $1007\text{ cm}^{-1}$  were assigned to the C-O stretching. The GC-mass spectrum of (**55**) showed a molecular ion at  $m/z$  172 which corresponded to  $\text{C}_{10}\text{H}_8\text{N}_2\text{O}$ . Whereas (**56**) and (**57**) showed a base peak at  $m/z$  186 which in well agreement with the molecular formula  $\text{C}_{11}\text{H}_{10}\text{N}_2\text{O}$ .



The  $^1\text{H}$  NMR spectra of compounds (**55**), (**56**) and (**57**) showed similar peaks in the region  $\delta$  8.33 –  $\delta$  8.03 which were due to the H-3, H-5 and H-6 of the pyrazine ring. Compound (**55**) showed the presence of monosubstituted benzene protons where four contiguous aromatic hydrogens were observed. A doublet of doublets at  $\delta$  7.38 with coupling constant of 4 Hz, 2.2 Hz and a doublet at  $\delta$  7.12 with coupling constant of 8 Hz were attributed to H-2', H-6' and H-3', H-5' respectively. In addition, a triplet which was detected at  $\delta$  7.21 with  $J$  value of 7.5 Hz was assigned to H-4' of the benzene

ring. The  $^1\text{H}$  NMR spectrum of **(56)** showed the doublet of doublets at  $\delta$  7.18 with coupling constant of 11.8 Hz and 7.5 Hz which was assigned to H-6', whereas singlet and multiplet were recorded at  $\delta$  6.98 and  $\delta$  6.87 which were assigned to H-2', H-5' and H-4' of the *m*-cresol ring. The  $^1\text{H}$  NMR spectrum of **(57)** on the other hand showed a pair of doublets at  $\delta$  7.21 and  $\delta$  7.02 with each of the doublet having a coupling constant of 8 Hz which were assigned to H-2', H-6' and H-3', H-5'. The symmetrical peaks indicated the characteristic of *para* disubstituted aromatic ring. A singlet recorded at  $\delta$  2.30, was believed to arise from the proton resonance on methyl group for both compound of **(56)** and **(57)**.

The  $^{13}\text{C}$  NMR spectrum of **(55)** indicated the presence of 10 carbons in the molecule, whereas  $^{13}\text{C}$  NMR spectra of **(56)** and **(57)** showed 11 carbons in agreement with the molecular formula. The spectrum of **(55)** showed peaks at  $\delta$  160.1 and  $\delta$  152.9 which were assigned to carbons on C-1' and C-2 of the benzene ring and pyrazine respectively. While carbon resonances recorded at  $\delta$  141.0,  $\delta$  138.4 and  $\delta$  135.8 were assigned to C-3, C-5 and C-6 of the pyrazine ring. Similar peaks were observed in spectra of **(56)** and **(57)** except the presence of an additional peak at  $\delta$  21.3 and  $\delta$  20.7, which were assigned to the carbon of the methyl group in both compounds.

Recrystallisation of **(55)** from chloroform gave block crystals, whereby crystal structure was analysed by X-ray diffraction method. The colourless crystals of **(55)** showed the dihedral angle between the aromatic rings which is  $64.2 (1)^\circ$  and the bridging C-O-C angle is  $119.1 (1)^\circ$ . The irregular block crystal of **(53)** presented in Figure 3.9 has a monoclinic system with space group  $P2_1/c$ .<sup>115</sup> The crystals system and refinement data are shown in Table 3.4.

The crystals system and refinement data of compound (**55**) are shown in Table 3.4

**Table 3.4: Crystal data and structure refinement for 2-phenoxy pyrazine (**55**)**

Identification code	Phenyl pyrazin-2-yl ether
Empirical formula	C <sub>10</sub> H <sub>8</sub> N <sub>2</sub> O
Formula weight	172.18
Colour	colourless
Crystal system, space group	Monoclinic, P2 <sub>1</sub> /c
Unit cell dimensions	$a = 5.704 (1) \text{ \AA}$ $b = 8.557 (2) \text{ \AA}$ $c = 17.595 (4) \text{ \AA}$ $\beta = 94.382 (3)^\circ$
$V (\text{\AA}^3)$	856.4 (3)
$Z$	4
$\rho_{\text{calc}}$ (Mg m <sup>-3</sup> )	1.335
Absorption coefficient (mm <sup>-1</sup> )	0.09
$F(000)$	360
Crystal size (mm)	0.20 x 0.15 x 0.10
$\theta_{\text{max}}$	26.1°
$\leq h \leq$	-6 to 7
$\leq k \leq$	-11 to 10
$\leq l \leq$	-22 to 21
Reflections collected / unique	4641 / 1950
$R_{\text{int}}$	0.042
Completeness to theta	2.3 – 27.5
Data / parameters	1950 / 118
Goodness-of-fit on $F^2$	0.046
Final $R$ indices [ $I > 2\sigma(I)$ ]	0.119

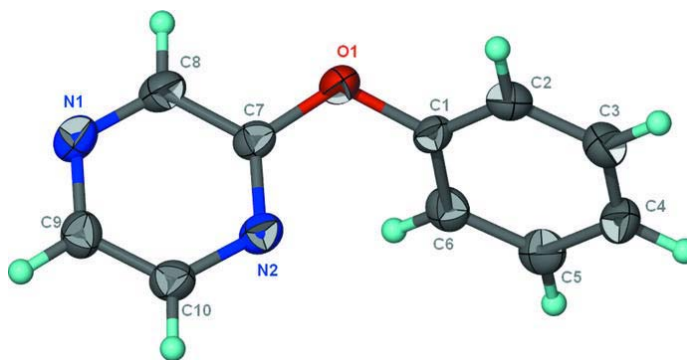


**Figure 3.9: Ortep diagram of 2-phenoxy pyrazine (**55**)**

### 3.3 Synthesis of quinoxaline derivatives

#### 3.3.1 Reactions of 2-chloroquinoxaline with piperidine and its derivatives

Reactions of 2-chloroquinoxaline (**58**) with piperidine (**34**), 3-methylpiperidine (**35**) and 4-methylpiperidine (**36**) were studied and as shown in Figure 3.10.

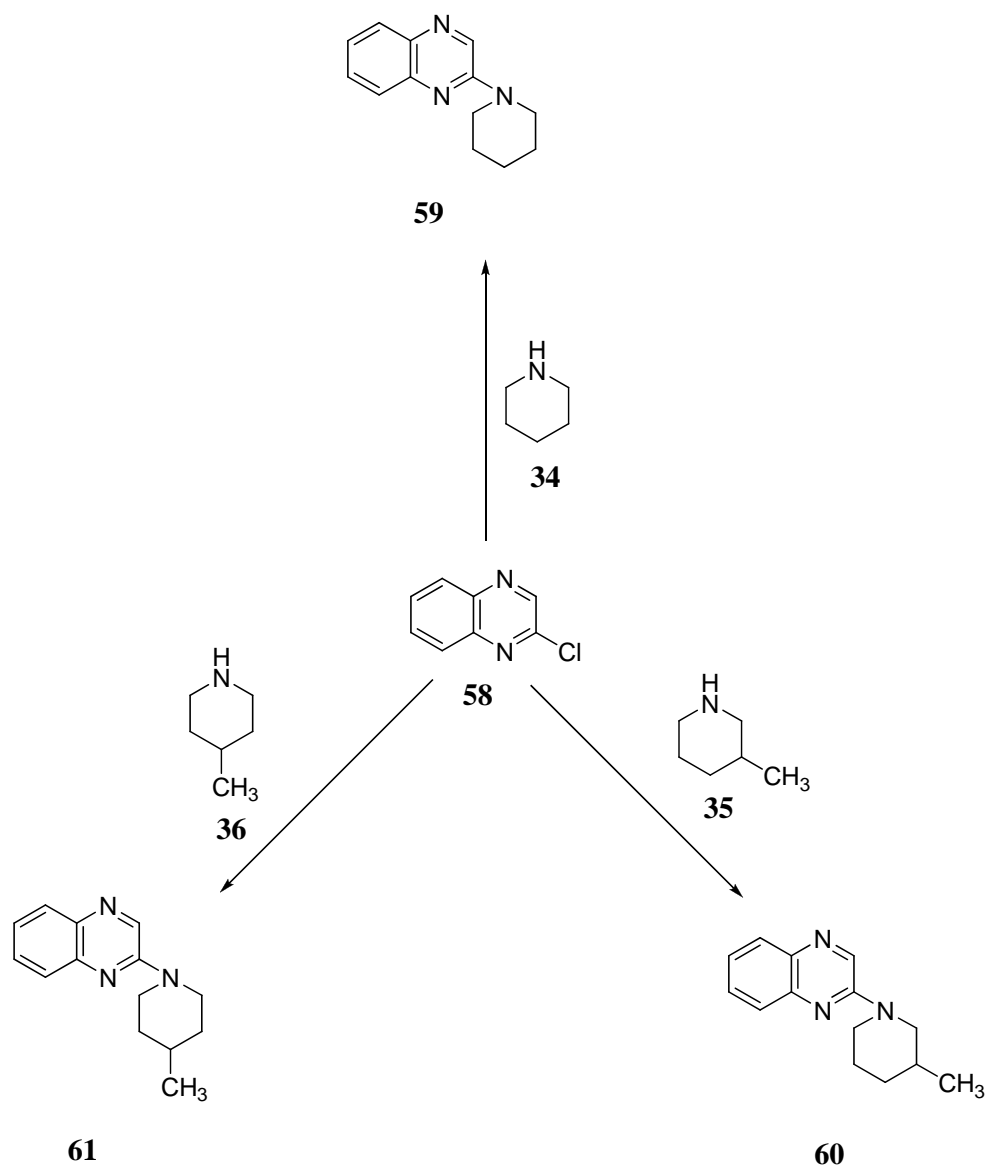
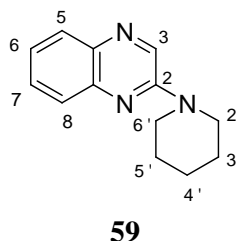


Figure 3.10: Reactions of 2-chloroquinoxaline with piperidine and its derivatives

Reaction of 2-chloroquinoxaline (**58**) with piperidine (**34**) gave 2-*N*-piperidinoquinoxaline (**59**) with 83%. The IR spectrum of (**59**) showed medium and strong bands at 1553 cm<sup>-1</sup> and 1582 cm<sup>-1</sup> respectively, which were due to the presence of C=N and C=C stretching. A strong absorption band was also observed at 2973 cm<sup>-1</sup>, which was due to C-H stretching. The molecular weight was indicated by the molecular ion at *m/z* 213 [M<sup>+</sup>] corresponds to the molecular formula C<sub>13</sub>H<sub>15</sub>N<sub>3</sub>.

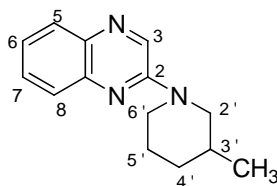


The <sup>1</sup>H NMR spectrum of (**59**) showed a singlet at δ 8.57. This was due to the proton resonance at H-3 of the quinoxaline ring. Doublets were observed at δ 7.83 and δ 7.64 with coupling constant of 8 Hz were corresponded to H-8 and H-5. Multiplets were observed at δ 7.52 and δ 7.33 which were assigned to H-7 and H-6 of the same ring. The most deshielded singlet signal in the upfield region recorded at δ 3.76 was assigned to H-2' and H-6'. In addition, a broad singlet peak was observed at δ 1.71 and the integration suggesting that there were six protons which probably due to the proton resonances at H-3', H-4' and H-5'.

The <sup>13</sup>C NMR spectrum indicated the presence of 13 carbons which consist of three quaternary carbons, five methine carbons and five methylene carbons in agreement with the molecular formula of (**59**). The quaternary carbon signals were recorded at δ 152.4, δ 141.8 and δ 136.4 which were assigned to C-2, C-10 and C-9. The signals at δ 136.0 – δ 124.2 in the downfield region were attributable to the C-3,

C-8, C-5, C-7 and C-6. Three peaks observed at  $\delta$  45.8,  $\delta$  25.6 and  $\delta$  24.6 were believed to arise from carbon resonances of C-2', C-6', C-3', C-5' and C-4'.

Reaction of 2-chloroquinoxaline (**58**) with 3-methylpiperidine (**35**) was also carried out with the method similar to that (**59**) and the structure of (**60**) was confirmed using the same methods. The IR spectrum showed absorption peaks similar to compound (**59**) as discussed earlier. The GC-mass spectrum showed a molecular ion at  $m/z$  227 corresponding to the molecular formula  $C_{14}H_{17}N_3$ .

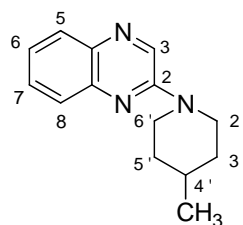


**60**

The  $^1H$  NMR spectrum of (**60**) showed peaks similar to the piperidino derivatives discussed in section 3.2.1. However, for compound (**60**), a triplet peak was recorded at  $\delta$  4.33 with coupling constant of 3.4 Hz which was assigned to H-6'. Triplet of doublets were observed at  $\delta$  2.89 with coupling constant of 12 Hz, 2.9 Hz which was corresponded to H-2'. A triplet at  $\delta$  2.56 with a coupling constant of 2.4 Hz was assigned to H-2'. Two multiplets were observed at  $\delta$  1.52 and  $\delta$  1.13 which were assigned to protons on H-4', H-5' and H-3'. A signal characteristic of methyl group was observed at  $\delta$  0.91 with  $J$  value of 8 Hz.

The  $^{13}\text{C}$  NMR spectrum of **(60)** showed a total of 14 carbons which is in agreement with the molecular formula of **(60)**. The signals at  $\delta$  152.4 –  $\delta$  124.3 in the downfield region were assigned to the carbons of the quinoxaline ring. Meanwhile, absorption peaks observed in the upfield region at  $\delta$  52.5 –  $\delta$  25.1 were assigned to carbons of the 3-methylpiperidine ring. A signal at  $\delta$  19.3 was believed to arise from the carbon resonance of the methyl group.

2-*N*-(4-Methyl)piperidinoquinoxaline **(61)** was obtained with a yield of 96% when 2-chloroquinoxaline **(58)** was treated with 4-methylpiperidine **(36)**. The IR spectrum of **(61)** was most identical to those of **(59)** and **(60)**, whereby strong and medium absorption bands at  $1551\text{ cm}^{-1}$  and  $1578\text{ cm}^{-1}$  corresponding to C=N and C=C stretches, a strong absorption band at  $2923\text{ cm}^{-1}$  correspond to C-H stretch. The mass spectrum showed a  $[\text{M}^+]$  peak at  $m/z$  227 corresponding to the molecular formula  $\text{C}_{11}\text{H}_{11}\text{N}_3$ .



**61**

The  $^1\text{H}$  NMR spectrum recorded proton peaks between  $\delta$  8.49 –  $\delta$  7.24 which was the pattern for proton resonances of the quinoxaline ring as discussed earlier. A doublet which was observed at  $\delta$  4.42 with  $J$  value of 8 Hz was corresponded to H-2'. Multiplet and triplet which were recorded at  $\delta$  2.86 and  $\delta$  1.68 with coupling constant of 1.2 Hz were assigned to H-6' and H-3'. H-4' and H-5' were recorded as multiplets at  $\delta$  1.53 and  $\delta$  1.12. In addition, a doublet at  $\delta$  0.88 with  $J$  value of 8 Hz was attributed to protons on the methyl group.

The  $^{13}\text{C}$  NMR spectrum of **(61)** showed 12 carbon resonances have a total of 14 carbon atoms which in agreement with the molecular formula of **(61)**. Carbon resonances in the downfield region at  $\delta$  152.2 –  $\delta$  124.1 were assigned to C-2, C-10, C-9, C-3, C-8, C-5, C-7 and C-6 of the quinoxaline ring. Whereas, peaks in the upfield region at  $\delta$  45.0,  $\delta$  33.7 and  $\delta$  31.1 were assigned to C-6', C-2', C-5', C-3' and C-4' respectively. The carbon resonance of methyl group was recorded at  $\delta$  21.7.

### 3.3.2 Reactions of 2-chloroquinoxaline with aniline and its derivatives

Reaction of 2-chloroquinoxaline (**58**) with aniline (**40**), *m*-toluidine (**41**), *p*-toluidine (**42**), *m*-anisidine (**43**), *p*-anisidine (**44**) and *p*-chloroaniline (**45**) were studied. Figure 3.11 shows a diagrammatic representation of the various reactions.

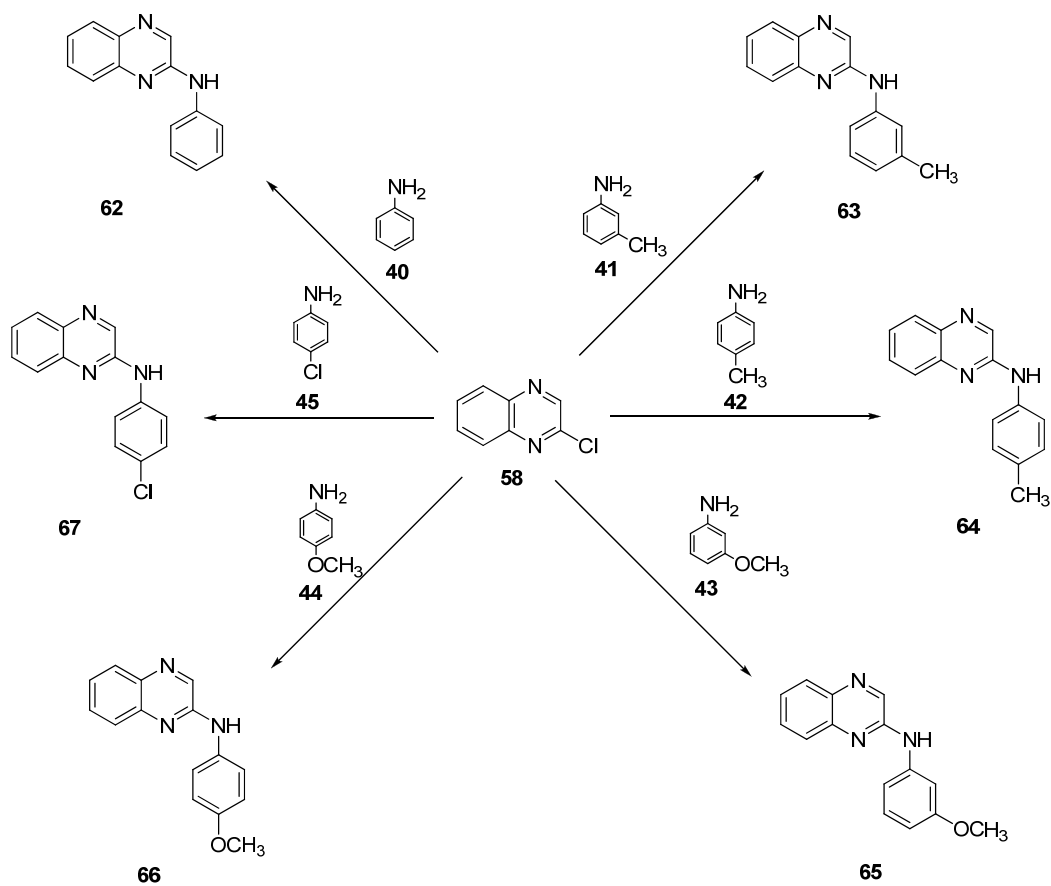
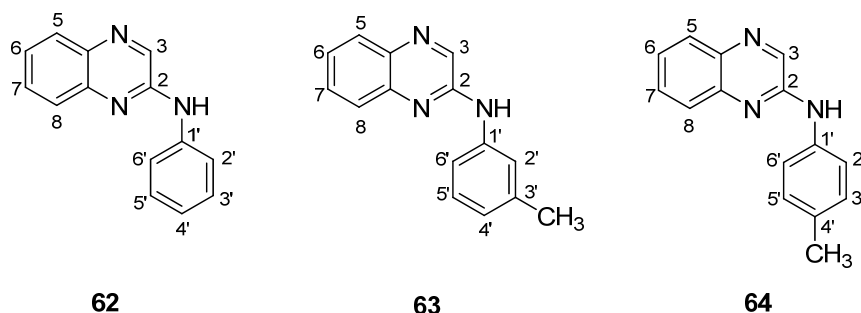


Figure 3.11: Reactions of 2-chloroquinoxaline with aniline and its derivatives

Reaction of 2-chloroquinoxaline (**58**) with aniline (**40**), *m*-toluidine (**41**) and *p*-toluidine (**42**) yielded 2-*N*-anilinoquinoxaline (**62**), 2-*N*-(*m*-methyl)anilinoquinoxaline (**63**) and 2-*N*-(*p*-methyl)anilinoquinoxaline (**64**), respectively.

The IR spectra of these compounds showed almost similar absorption peaks which corresponded to C=N, aromatic C=C and N-H stretches. Compound (**62**) showed a weak and a strong absorption bands at 691 cm<sup>-1</sup> and 749 cm<sup>-1</sup> indicating a monosubstituted benzene ring. Compound (**63**) on the other hand showed strong and medium absorption bands at 760 cm<sup>-1</sup> and 786 cm<sup>-1</sup>, corresponding to meta disubstituted aromatic ring. A medium absorption band at 817 cm<sup>-1</sup> showed para disubstituted aromatic ring of compound (**64**). The mass spectrum of (**62**) gave a [M<sup>+</sup>] peak at *m/z*. 221 corresponding to the molecular formula C<sub>14</sub>H<sub>11</sub>N<sub>3</sub> while mass spectra of (**63**) and (**64**) gave molecular ion at *m/z* 235, yielded the molecular formula C<sub>15</sub>H<sub>13</sub>N<sub>3</sub>.



The <sup>1</sup>H NMR spectra of all the compounds showed similar peaks in the region of δ 8.39 – δ 7.41 which were assigned to H-3, H-8, H-5, H-7 and H-6. <sup>1</sup>H NMR of spectrum (**62**) showed a doublet at δ 7.72 with a coupling constant of 8 Hz which corresponded to H-2' and H-6'. Pair of triplets were recorded at δ 7.38 and δ 7.11 with *J* value of 8.2 Hz and 7.6 Hz which were assigned to H-3', H-5' and H-4', while compound (**63**) showed a singlet at δ 7.41 which was assigned to H-2'. Triplets at δ 7.37 and δ 7.19 with *J* value of 6.8 Hz and 7.8 Hz which corresponded to H-6' and

H-4', H-5'.  $^1\text{H}$  NMR of spectrum (**64**) showed the symmetrical doublets at  $\delta$  7.53 and  $\delta$  7.17 with  $J$  value of 8 Hz that gave a characteristic of *para* disubstituted ring. Compounds (**63**) and (**64**) showed an additional singlet which resulted from the protons on methyl group. A broad singlet recorded at  $\delta$  6.87 –  $\delta$  6.90 was assigned to the proton of NH group.

The  $^{13}\text{C}$  NMR spectrum of (**62**) indicated the presence of 14 carbons in the molecule, whereas spectra of compound (**63**) and (**64**) showed 15 carbons in agreement with the molecular formula. The spectrum of (**62**) showed peaks in the region of  $\delta$  149.2 –  $\delta$  119.9 which were assigned to carbons on quinoxaline and aniline rings. Similar peaks were also observed in spectra of (**63**) and (**64**) except an additional peaks at  $\delta$  21.5 for (**63**) and  $\delta$  20.8 for (**64**), which were assigned to the methyl carbon of both compounds. The full assignments of spectra  $^{13}\text{C}$  NMR for compound (**62**), (**63**), and (**64**) can be obtained in Chapter 5.

Recrystallisation of 2-*N*-(*p*-methyl)anilinoquinoxaline (**64**) from chloroform gave yellowish well shaped crystals which were analysed by X-ray diffraction method. The crystal (**64**) has an orthorhombic system, *Pbca*. The aromatic and the aromatic fused-rings in compound (**64**), open the angle at the planar N atom to 130.07 (13) $^\circ$  and 129.98 (13) $^\circ$  in the two independent molecules in the asymmetric unit. The amino N atom of one molecule forms a hydrogen bond to the 4-N atom of an adjacent quinoxaliny ring, generating a supramolecular chain.<sup>116</sup> The crystals system and refinement data are shown in Table 3.5. Figure 3.12 shows the thermal ellipsoid plot for the two independent molecules of compound (**64**) at the 70% probability level, hydrogen atoms are drawn as spheres of arbitrary radius.

The crystals system and refinement data are shown in Table 3.5

**Table 3.5: Crystal data and structure refinement for 2-*N*-(*p*-methyl)anilinoquinoxaline (64)**

Identification code	<i>N</i> -(Quinoxalin-2-yl)-4-toluidine
Empirical formula	C <sub>15</sub> H <sub>13</sub> N <sub>3</sub>
Formula weight	235.28
Colour	yellow
Crystal system, space group	Orthorhombic, <i>Pbca</i>
Unit cell dimensions	<i>a</i> = 12.2081 (9) Å <i>b</i> = 11.3720 (9) Å <i>c</i> = 35.097 (3) Å $\lambda$ = 0.71073 Å
<i>V</i> (Å <sup>3</sup> )	4872.5 (6)
<i>Z</i>	16
$\rho_{\text{calc}}$ (Mg m <sup>-3</sup> )	1.283
Absorption coefficient (mm <sup>-1</sup> )	0.08
<i>F</i> (000)	1984
Crystal size (mm)	0.40 x 0.15 x 0.05
$\theta_{\text{max}}$	27.5°
$\leq h \leq$	-15 to 15
$\leq k \leq$	-14 to 9
$\leq l \leq$	-45 to 45
Reflections collected / unique	26747/ 5592
<i>R</i> <sub>int</sub>	0.051
Completeness to theta	31.2 – 27.5
Data / restraints / parameters	5592/ 2/ 335
Goodness-of-fit on <i>F</i> <sup>2</sup>	0.041
Final <i>R</i> indices [ <i>I</i> > 2σ ( <i>I</i> )]	0.112

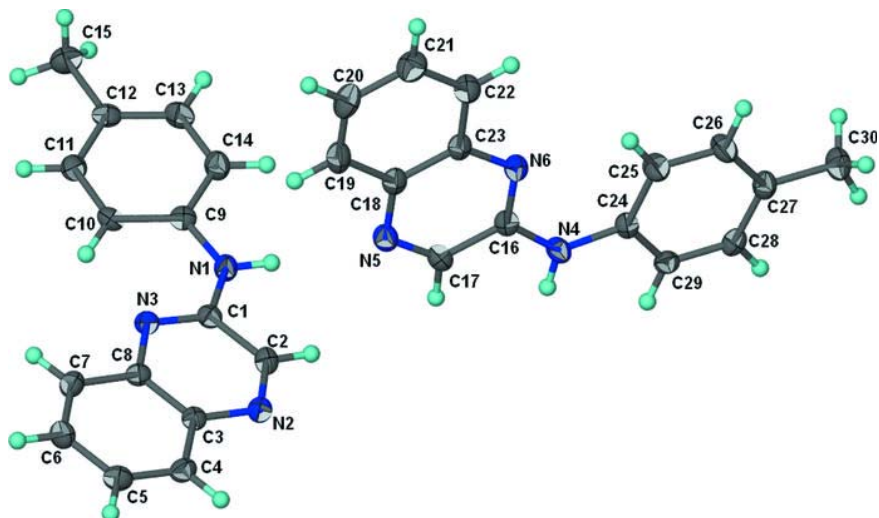
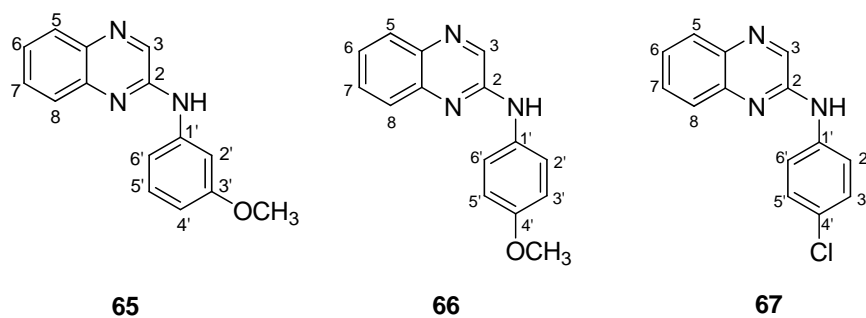


**Figure 3.12: Ortep diagram of 2-*N*-(*p*-methyl)anilinoquinoxaline (64)**

Reactions of 2-chloroquinoxaline (**58**) with *m*-anisidine (**43**), *p*-anisidine (**44**) and *p*-chloroaniline (**45**) gave 2-*N*-(*m*-methoxy)anilinoquinoxaline (**65**) which is brown, 2-*N*-(*p*-methoxy)anilinoquinoxaline (**66**) is green solid and 2-*N*-(*p*-chloro)anilinoquinoxaline (**67**) which is colourless.

The infrared spectra of (**65**), (**66**) and (**67**) showed similar absorptions to those of aniline derivatives as discussed earlier. Spectrum of (**65**) showed the strong and weak absorption bands which gave the characteristic of meta disubstituted ring at  $759\text{ cm}^{-1}$  and  $832\text{ cm}^{-1}$  while (**66**) and (**67**) showed a strong absorption band at  $822\text{ cm}^{-1}$  and  $828\text{ cm}^{-1}$  respectively, which indicating the characteristic of *para* disubstituted aromatic ring. The GC-mass spectra of (**65**) and (**66**) showed a molecular ion at  $m/z$  201, which corresponded to  $\text{C}_{11}\text{H}_{11}\text{N}_3\text{O}$ . Meanwhile, (**67**) showed a molecular ion at  $m/z$  255, consistent with the molecular formula  $\text{C}_{14}\text{H}_{10}\text{N}_3\text{Cl}$ .



The  $^1\text{H}$  NMR spectra of (**65**), (**66**) and (**67**) showed proton coupling of the quinoxaline ring at  $\delta$  8.37 –  $\delta$  7.37 as discussed earlier. Compounds (**66**) and (**67**) showed a distinguish broad singlet attributed to NH at  $\delta$  1.87 and  $\delta$  6.91 respectively. However, the NH peak did not appear in (**65**). The protons on methoxy group for compound (**65**) and (**66**) can be clearly observed as a singlet at  $\delta$  3.74 and  $\delta$  3.80 respectively.

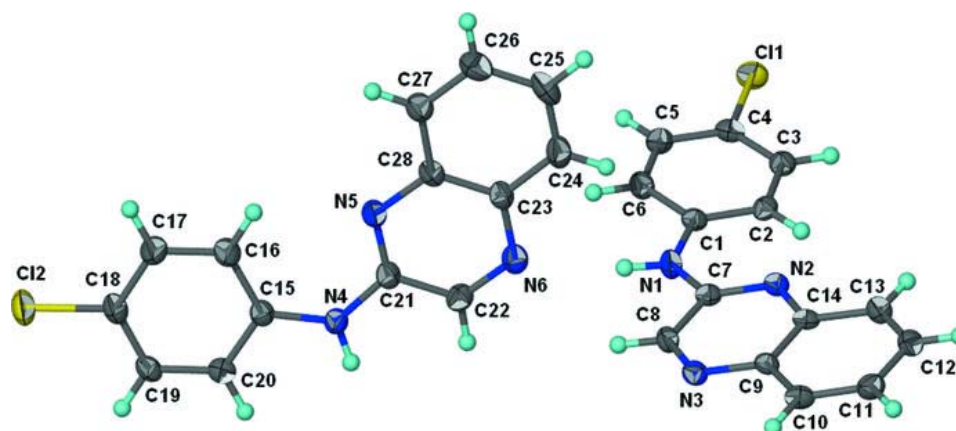
The  $^{13}\text{C}$  NMR spectra of **(65)** and **(66)** indicated the presence of 15 carbons which consist of five quaternary carbons, nine methine carbons and one methyl while **(67)** had a total of 14 carbons which consist of five quaternary carbons and nine methine carbons. The  $^{13}\text{C}$  NMR spectra of these compounds showed peaks similar to the previous aniline derivatives except for **(65)** and **(66)**, an additional peak was recorded at  $\delta$  55.3 -  $\delta$  55.5 which were assigned to the methoxy group.

Recrystallisation of **(67)** from chloroform gave colourless prisms where the crystal structure was analysed using X-ray diffraction method. The crystal **(67)** has an orthorhombic system, *Pbca*. There were two molecules in the asymmetric unit of the compound with dihedral angles of 5.11 (10) and 13.61 (10) $^\circ$  between the aromatic ring systems. In the crystal structure, the molecules were linked by N-H---N hydrogen bonds, resulting in chain propagating in [010].<sup>117</sup> The crystals system and refinement data are shown in Table 3.6. Figure 3.13 showed the crystal structure of **(67)** at the 70% probability level, whereby hydrogen atoms were drawn as spheres of arbitrary radius.

The crystals system and refinement data are shown in Table 3.6

**Table 3.6: Crystal data and structure refinement for 2-*N*-(*p*-chloro)anilinoquinoxaline (67)**

Identification code	2-(4-Chloroanilino)quinoxaline
Empirical formula	C <sub>14</sub> H <sub>10</sub> ClN <sub>3</sub>
Formula weight	255.70
Colour	colourless
Crystal system, space group	Orthorhombic, <i>Pbca</i>
Unit cell dimensions	$a = 12.155 (1) \text{ \AA}$ $b = 11.238 (1) \text{ \AA}$ $c = 35.421 (3) \text{ \AA}$ $\lambda = 0.71073 \text{ \AA}$
$V (\text{\AA}^3)$	4838.3 (8)
$Z$	16
$\rho_{\text{calc}}$ (Mg m <sup>-3</sup> )	1.404
Absorption coefficient (mm <sup>-1</sup> )	0.30
$F(000)$	2112
Crystal size (mm)	0.30 x 0.20 x 0.10
$\theta_{\text{max}}$	27.8°
$\leq h \leq$	-15 to 15
$\leq k \leq$	-14 to 14
$\leq l \leq$	-34 to 45
Reflections collected / unique	25622 / 5495
$R_{\text{int}}$	0.066
Completeness to theta	2.5 – 27.8
Data / restraints / parameters	5495 / 2 / 331
Goodness-of-fit on $F^2$	0.058
Final $R$ indices [ $I > 2\sigma(I)$ ]	0.135

**Figure 3.13: Ortep diagram of 2-*N*-(*p*-chloro)anilinoquinoxaline (67)**

### 3.3.3 Reactions of 2-chloroquinoxaline with phenol and cresols

Reactions of 2-chloroquinoxaline (**58**) with phenol (**52**), *m*-cresol (**53**) and *p*-cresol (**54**) were studied and as shown in Figure 3.14.

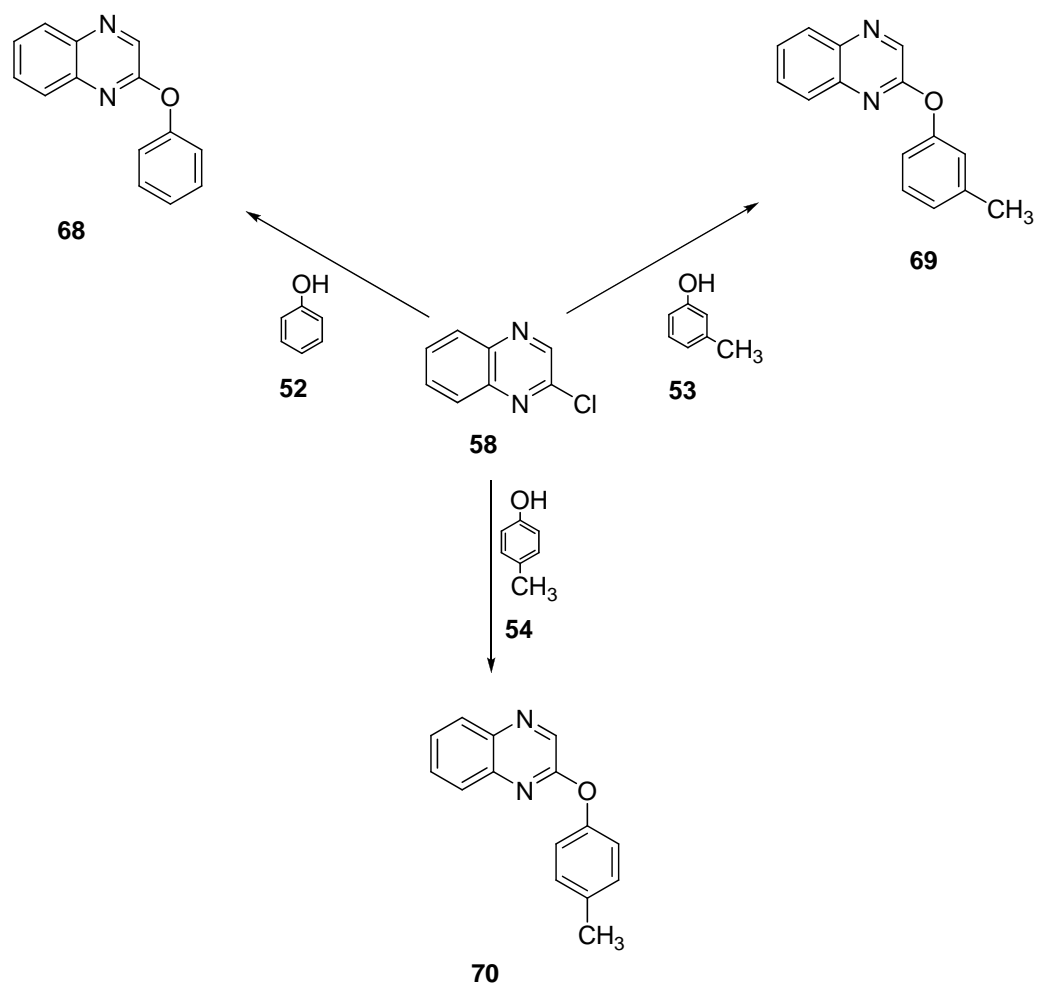
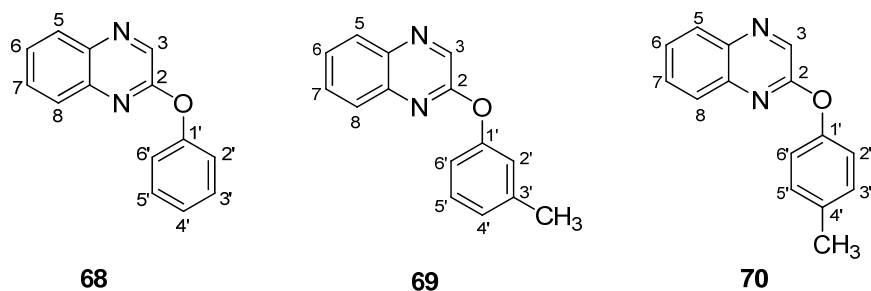


Figure 3.14: Reactions of 2-chloroquinoxaline with phenol and cresols

Reactions of 2-chloroquinoxaline (**58**) with phenol (**52**), *m*-cresol (**53**) and *p*-cresol (**54**) gave 2-phenoxyquinoxaline (**68**), 2-(*m*-methyl)phenoxyquinoxaline (**69**) and 2-(*p*-methyl)phenoxyquinoxaline (**70**) respectively with percentage yields of more than 60%.

The infrared spectra of (**68**), (**69**) and (**70**) showed similar absorptions to those of phenoxy derivatives as mentioned earlier. Spectrum of (**68**) showed both medium and strong absorption bands at  $689\text{ cm}^{-1}$  and  $761\text{ cm}^{-1}$  indicating a monosubstituted benzene ring. Meanwhile, (**69**) showed two bands at  $778\text{ cm}^{-1}$  and  $826\text{ cm}^{-1}$  indicating the characteristic of *meta* disubstituted ring. Compound (**70**) showed the strong absorption peak at  $825\text{ cm}^{-1}$  that gave the characteristic of *para* disubstituted ring. The GC-mass spectrum of (**68**) showed a molecular ion at  $m/z$  222, consistent with the molecular formula  $\text{C}_{14}\text{H}_{10}\text{N}_2\text{O}$ . Meanwhile, (**69**) and (**70**) showed a molecular ion at  $m/z$  236, which corresponded to  $\text{C}_{15}\text{H}_{12}\text{N}_2\text{O}$ .



The  $^1\text{H}$  NMR spectra of (**68**), (**69**) and (**70**) showed similar absorption peaks as quinoxaline derivatives in the regions of  $\delta$  8.68 -  $\delta$ 7.51. The spectrum of (**68**) showed the presence of five aromatic hydrogens at  $\delta$  7.36 as triplet of doublets (td) with  $J$  value of 7.6 Hz and 1.6 Hz and a multiplet at  $\delta$  7.18 which were assigned to the protons on H-2', H-6' and H-3', H-5', H-4' of the benzene ring. Compound (**69**) showed triplet of doublets (td) and a triplet at  $\delta$  7.25 and  $\delta$  7.00 with coupling constant of 7.3 Hz, 1.4 Hz

and 7.5 Hz which were due to the resonance of protons of H-2', H-6' and H-3', H-5' of *m*-cresol. <sup>1</sup>H NMR spectrum of **(70)** showed doublets at δ 7.26 and δ 7.00 with a coupling constant of 8 Hz and 8 Hz indicating the protons of H-2', H-6' and H-3', H-5' of the *p*-cresol ring. For **(69)** and **(70)**, a singlet was observed at δ 2.40 – δ 2.31 which corresponded to the proton resonances of the methyl group.

The <sup>13</sup>C NMR spectrum of **(68)** indicated the presence of 14 carbons, whereas <sup>13</sup>C NMR spectra of **(69)** and **(70)** showed 15 carbons in agreement with their molecular formula. The quaternary carbons of **(68)** were observed at δ 156.9, δ 152.7, δ 139.9 and δ 139.6 were attributed to C-2, C-1', C-10 and C-9. The signals at δ 129.6 and δ 121.3 were assigned to C-2', C-6' and C-3', C-5' of the benzene ring. The <sup>13</sup>C NMR spectra of **(69)** and **(70)** also showed peaks similar to that of **(68)** except an additional peak recorded at about δ 21.4 - δ 20.9, which was due to the resonance of methyl group carbon. The full assignments of spectra <sup>13</sup>C NMR for **(68)**, **(69)** and **(70)** are also summarised in Chapter 5.

### 3.4 Fluorescence characteristics

In order to effectively utilize luminescence as an analytical tool, it is necessary to know the basic effects of structure and the environment on the emission process. The fluorescence of a molecule depends on its structure and on the environment in which the luminescence is measured. Under structural effects, the types of compounds fluoresce and how to increase the total emission by changes in structure need to be considered. On environmental effects, we studied how solvent, oxygen, substituents, pH and other variable affect the luminescence characteristics of compounds.

In this study, molecules of particular interest are the nitrogen heterocyclics. In general, the introduction of a nitrogen atom into an aromatic ring system reduces fluorescence. In addition, the presence of second nitrogen, =N- in the system diminishes fluorescence further. The work started with the study of the fluorescence of pyrazine derivatives followed by its fused system, quinoxaline derivatives with respect to chemical structure and environmental effects.

The effect of substituents on the fluorescence of benzene has been studied by Stevenson<sup>118</sup> in 1965. Pyrazine and quinoxaline derivatives that contain of benzene ring with electron donating substituents usually exhibit a considerable amount of fluorescence. Some of these compounds fluoresce intensely in certain solvents, concentrations, pH and other variable as mentioned earlier.

Table 3.7 and Table 3.8 show the fluorescence characteristic of 2-*N*-piperidinopyrazine (**37**) and 2-*N*-anilinopyrazine (**46**) in various solvents in capped and uncapped conditions.

**Table 3.7: Fluorescence characteristic of 2-*N*-piperidinopyrazine (**37**) in various solvents ( $6.127 \times 10^{-6}$  M)**

Condition	Solvent	Excitation wavelength (nm)	Fluorescence wavelength (nm)	Intensity
Capped	Tetrahydrofuran	345	403	62.27
	Acetonitrile	348	411	51.64
	Ethyl acetate	344	404	26.3
	Ethanol	349	422	4.183
Uncapped	Tetrahydrofuran	345	402	60.30
	Acetonitrile	348	411	51.00
	Ethyl acetate	344	402	24.08
	Ethanol	349	418	3.895

**Table 3.8: Fluorescence characteristic of 2-*N*-anilinopyrazine (**46**) in various solvents ( $5.840 \times 10^{-6}$  M)**

Condition	Solvent	Excitation wavelength (nm)	Fluorescence wavelength (nm)	Intensity
Capped	Tetrahydrofuran	347	435	12.33
	Acetonitrile	348	386	2.257
	Ethyl acetate	334	379	5.258
	Ethanol	312	340	0.457
Uncapped	Tetrahydrofuran	347	434	11.55
	Acetonitrile	348	386	2.249
	Ethyl acetate	334	378	5.247
	Ethanol	312	339	0.442

The fluorescence spectra of 2-*N*-piperidinopyrazine (**37**) and 2-*N*-anilinopyrazine (**46**) in various solvents in capped condition are as shown in Figure 3.15 and Figure 3.16.

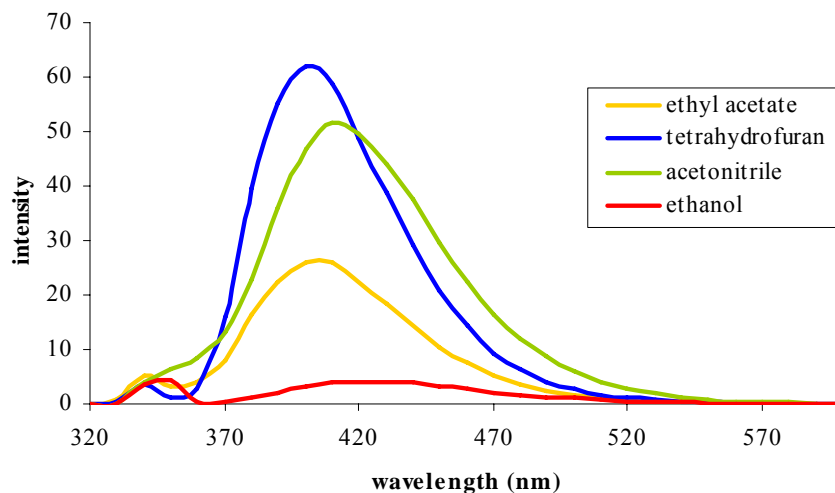


**Figure 3.15: Fluorescence spectra of 2-*N*-piperidinopyrazine (**37**) in various solvents in capped condition ( $6.127 \times 10^{-6}$  M)**

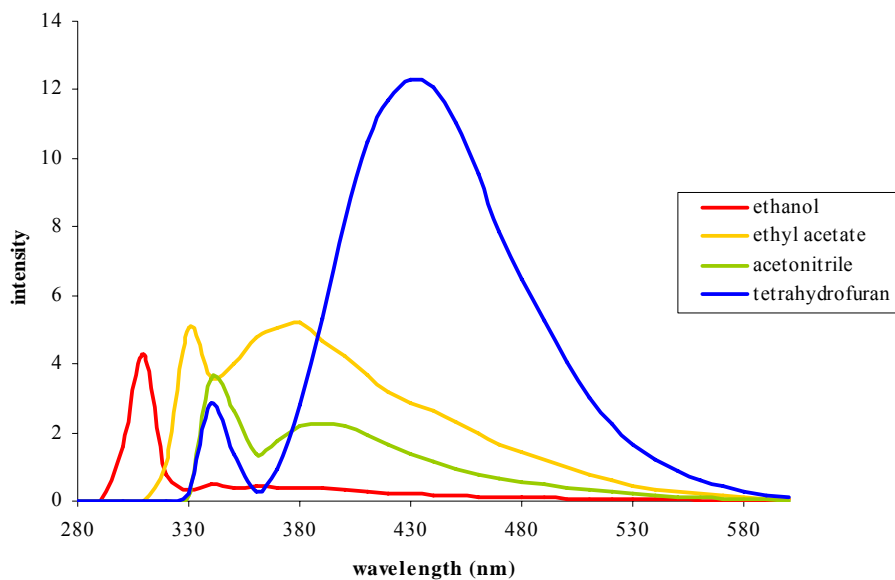


**Figure 3.16: Fluorescence spectra of 2-*N*-anilinopyrazine (**46**) in various solvents in capped condition ( $5.840 \times 10^{-6}$  M)**

It can be seen from Table 3.7 and Table 3.8, these compounds showed the highest fluorescence intensity in tetrahydrofuran followed by acetonitrile, ethyl acetate and ethanol. The fluorescence spectra were as shown in Figure 3.15 and Figure 3.16.

In most polar molecules, the excited state is more polar than the ground state. Hence, an increase in the polarity of the solvent produces a greater stabilisation of the excited state than of the ground state. Consequently, a shift in fluorescence spectra to longer wavelength is usually observed as the polar solvents and dielectric constant increases.<sup>109</sup> This phenomenon favours the shifting of emission maxima towards the higher wavelength as shown in Figure 3.15 and Figure 3.16. Compound **(37)** and **(46)** showed the higher shifting of fluorescence wavelength in THF and acetonitrile which both are polar aprotic solvent and have higher dielectric constant. This observation is in the agreement with the work done by Drobnik and Augenstein.<sup>119,120</sup>

Both 2-*N*-piperidinopyrazine **(37)** and 2-*N*-anilinopyrazine **(46)** showed the lowest fluorescence intensities in ethanol. The lowest fluorescence intensity observed in 2-*N*-piperidinopyrazine **(37)** and 2-*N*-anilinopyrazine **(46)** in ethanol is also believed to be due to the quenching effect from the “hydrogen bonded solvents” associated with the lone pair of electrons on the pyrazine ring and the amine group. As the result, it is not available to move around the system, thus low fluorescence intensity was observed. It is also believe that compound **(37)** and **(46)** formed a complex with the solvent as shown in Figure 3.17. It shows the formation of intramolecular charge transfer transitions via hydrogen bonding of compound **(37)** and **(46)**.

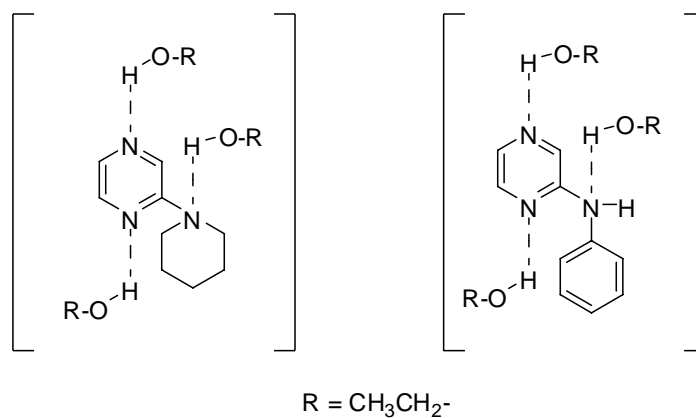


**Figure 3.17: Formation of hydrogen bonded of compound (37) and (46)**

This phenomenon is also explained by Weisstuch and Testa<sup>121</sup> which they had reported that in some aromatic heterocyclic compounds with hydrogen bonding formation would quench the fluorescence intensity. The formation of hydrogen bond which is capable of conjugating with the  $\pi$ -electron system of the heterocyclic ring, results in the mobility of the  $\pi$ -electron being disturbed and caused the fluorescence intensity to be reduced. This phenomenon favours the low lying  $n \rightarrow \pi^*$  transitions which refer to the excitation of a nonbonding electron to an antibonding orbital.<sup>122</sup> It was reported that  $n \rightarrow \pi^*$  transitions were usually not observed in fluorescence spectra and when present were weak.<sup>123</sup> As the results, a decrease in fluorescence intensity was observed.

Studies also show 2-*N*-piperidinopyrazine (**37**) is more fluorescent compared to 2-*N*-anilinopyrazine (**46**). This is probably due to the rigidity of the structure of 2-*N*-piperidinopyrazine (**37**) as shown in Figure 3.18, whereby compound (**37**) has no '-NH-' bridge as compared compound (**46**). Normally, a rigid structure reduced the vibrational amplitudes which promote radiationless losses which increase the fluorescence intensity.

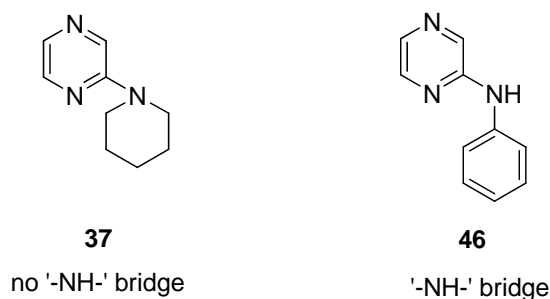


**Figure 3.18: Structures of 2-*N*-piperidinopyrazine (37) and 2-*N*-anilinopyrazine(46)**

2-*N*-Anilinopyrazine (**46**), on the other hand is a non-rigid structure, which has the capability of decreasing the fluorescence intensity due to the vibrational amplitudes. In addition, the formation of complex with the solvent through hydrogen bonding as suggested in Figure 3.17 may also increase the vibrational amplitude of the complex, thus energy absorbed was dissipated as heat.

Table 3.8 also shows the lower fluorescence intensity of 2-*N*-anilinopyrazine in ethyl acetate compare to in tetrahydrofuran. This is probably due to complex formed in ethyl acetate is less rigid than the complex formed in tetrahydrofuran. The -CH<sub>3</sub> and O-CH<sub>2</sub>CH<sub>3</sub> group of ethyl acetate may increase the vibrational amplitude of the complex and energy absorbed thus dissipated as heat and as the result low fluorescence intensity observed.

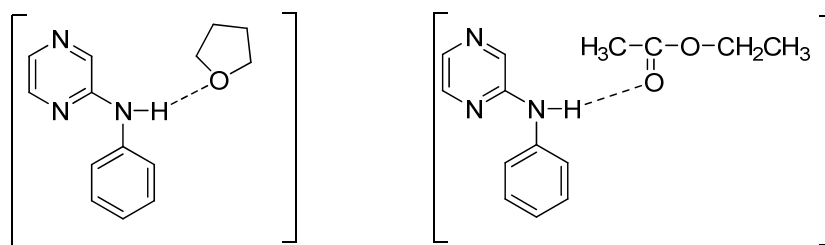


**Figure 3.19: Formation of complex in THF and ethyl acetate**

Table 3.9 and Table 3.10 show the fluorescence characteristics of 2- *N*-piperidinoquinoxaline (**59**) and 2-*N*-anilinoquinoxaline (**62**) in various solvents in capped and uncapped conditions.

**Table 3.9: Fluorescence characteristic of 2-*N*-piperidinoquinoxaline (**59**) in various solvents ( $4.6886 \times 10^{-6}$  M)**

Condition	Solvent	Excitation wavelength (nm)	Fluorescence wavelength (nm)	Intensity
Capped	Tetrahydrofuran	382	437	6.779
	Acetonitrile	383	446	17.38
	Ethyl acetate	380	438	8.822
	Ethanol	385	450	6.857
Uncapped	Tetrahydrofuran	382	437	6.667
	Acetonitrile	383	447	17.150
	Ethyl acetate	380	439	8.702
	Ethanol	385	453	6.7

2-*N*-Piperidinoquinoxaline (**59**) shows maximum fluorescence intensity in acetonitrile, followed by tetrahydrofuran, ethyl acetate and ethanol. The higher intensity in acetonitrile is believed to be due to the dielectric properties of the solvent. Acetonitrile is a polar aprotic solvent and its polarity produces a greater stabilization of the  $\pi$  to  $\pi^*$  excited state, thus increasing the fluorescence intensity.

**Table 3.10: Fluorescence characteristic of 2-*N*-anilinoquinoxaline (**62**) in various solvents ( $4.5195 \times 10^{-6}$  M)**

Condition	Solvent	Excitation wavelength (nm)	Fluorescence wavelength (nm)	Intensity
Capped	Tetrahydrofuran	380	485	2.303
	Acetonitrile	382	411	1.294
	Ethyl acetate	non-fluorescent		
	Ethanol	305	406	0.488
Uncapped	Tetrahydrofuran	380	483	2.220
	Acetonitrile	382	411	1.294
	Ethyl acetate	non-fluorescent		
	Ethanol	305	403	0.444

Table 3.9 shows the highest fluorescence intensity of 2-*N*-anilinoquinoxaline (**62**) in tetrahydrofuran, followed by in acetonitrile and ethanol for both capped and uncapped conditions. The observed fluorescence intensity of 2-*N*-anilinoquinoxaline (**62**) which is less fluorescent than 2-*N*-piperidinoquinoxaline (**59**) is believed to be due to the same reason as in the pyrazine system discussed earlier.

The fluorescence intensity of capped samples was observed to be higher than the uncapped samples as shown in the Table 3.7, 3.8, 3.9 and 3.10 for both systems. The low fluorescence intensity for uncapped sample is believed to be due to the unlimited amount of oxygen in the quartz cell. Oxygen which has an unusually large diffusion coefficient, on exposure of the solution to the atmosphere could result in large quantity of oxygen diffusing into solution and therefore quenched the fluorescence intensity of the compounds, thus reducing the fluorescence intensity.

The fluorescence spectra of 2-*N*-piperidinopyrazine (**37**), 2-*N*-piperidinoquinoxaline (**59**), 2-*N*-anilinopyrazine (**46**) and 2-*N*-anilinoquinoxaline (**62**) in THF and acetonitrile are as shown in Figure 3.20 and Figure 3.21.

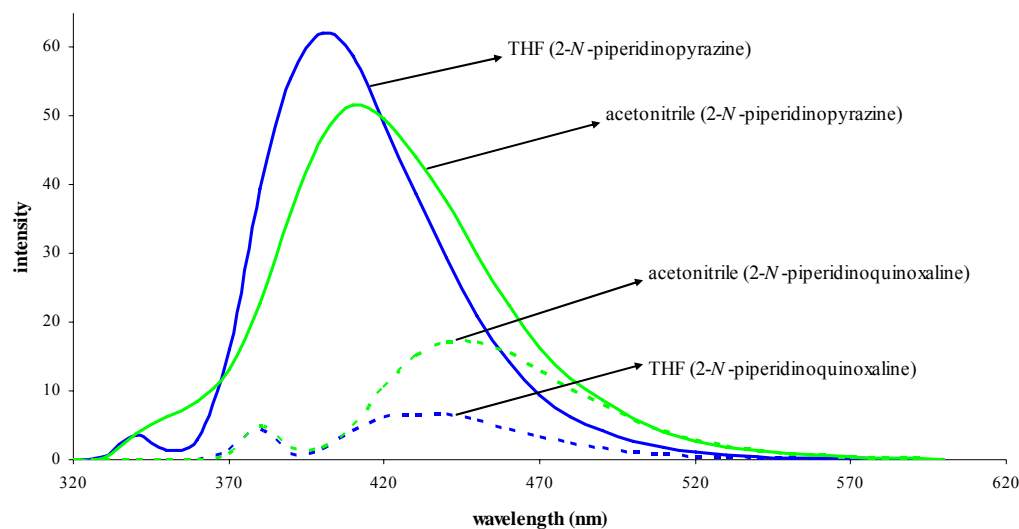


**Figure 3.20: Fluorescence spectra of 2-*N*-piperidinopyrazine (**37**) and 2-*N*-piperidinoquinoxaline (**59**) in THF and acetonitrile**

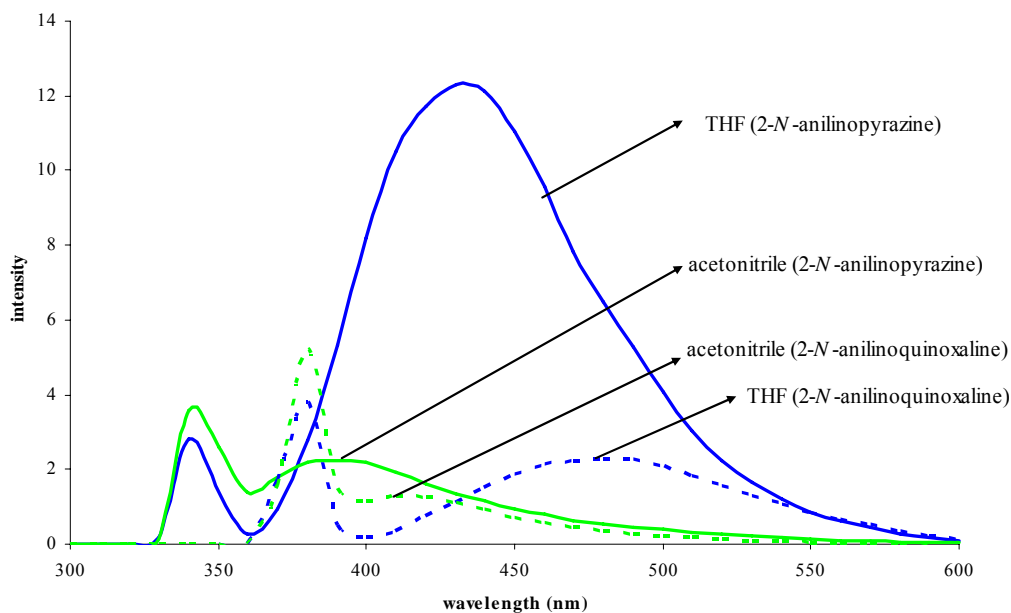


**Figure 3.21: Fluorescence spectra of 2-*N*-anilinopyrazine (**46**) and 2-*N*-anilinoquinoxaline (**62**) in THF and acetonitrile**

It can also be seen from Table 3.7 and Table 3.9 that 2-*N*-piperidinoquinoxaline (**59**) fluoresced at a higher wavelength compared to the 2-*N*-piperidinopyrazine (**37**). The same phenomenon was also observed with 2-*N*-anilinopyrazine (**46**) and 2-*N*-anilinoquinoxaline (**62**) as shown in Table 3.8 and Table 3.10. The shifting of emission maxima towards the higher wavelength as shown in Figure 3.20 and Figure 3.21 is due to the addition of benzene ring fused with pyrazine which enhanced the mobility on electrons through the  $\pi$  system in the benzene ring.<sup>109</sup>

Table 3.11 shows the fluorescence characteristic of 2-*N*-anilinopyrazine and 2-phenoxy pyrazine. Table 3.12 shows the fluorescence characteristic of 2-*N*-anilinoquinoxaline and 2-phenoxyquinoxaline in various solvents in capped condition respectively.

**Table 3.11: Fluorescence characteristic of 2-*N*-anilinopyrazine ( $5.8400 \times 10^{-4}$  M) and 2-phenoxy pyrazine ( $5.8079 \times 10^{-4}$  M) in various solvents in capped condition**

2-Y-pyrazine	Solvent	Excitation wavelength (nm)	Fluorescence wavelength (nm)	Intensity
- <i>N</i> -anilino ( <b>46</b> )	Tetrahydrofuran	370	432	97.55
	Acetonitrile	377	414	10.09
	Ethyl acetate	371	438	18.54
	Ethanol	399	496	1.78
-phenoxy ( <b>55</b> )	Tetrahydrofuran	387	434	0.262
	Acetonitrile	320	387	1.99
	Ethyl acetate	314	340	3.78
	Ethanol	X	X	X

X=non-fluorescent

**Table 3.12: Fluorescence characteristic of 2-*N*-anilinoquinoxaline ( $4.5195 \times 10^{-5}$  M) and 2-phenoxyquinoxaline ( $4.4996 \times 10^{-5}$  M) in various solvents in capped condition**

2-Y-quinoxaline	Solvent	Excitation wavelength (nm)	Fluorescence wavelength (nm)	Intensity
<i>-N</i> -anilino (62)	Tetrahydrofuran	382	483	14.07
	Acetonitrile	325	395	5.94
	Ethyl acetate	384	484	7.11
	Ethanol	305	335	0.59
<i>-phenoxy</i> (68)	Tetrahydrofuran	412	510	9.52
	Acetonitrile	380	448	2.42
	Ethyl acetate	404	506	4.66
	Ethanol	413	480	3.19

Figure 3.22 and Figure 3.23 show fluorescence spectra of 2-*N*-anilinoquinoxaline (46), 2-phenoxyquinoxaline (55), 2-*N*-anilinoquinoxaline (62) and 2-phenoxyquinoxaline (68) in ethyl acetate and acetonitrile in capped condition.

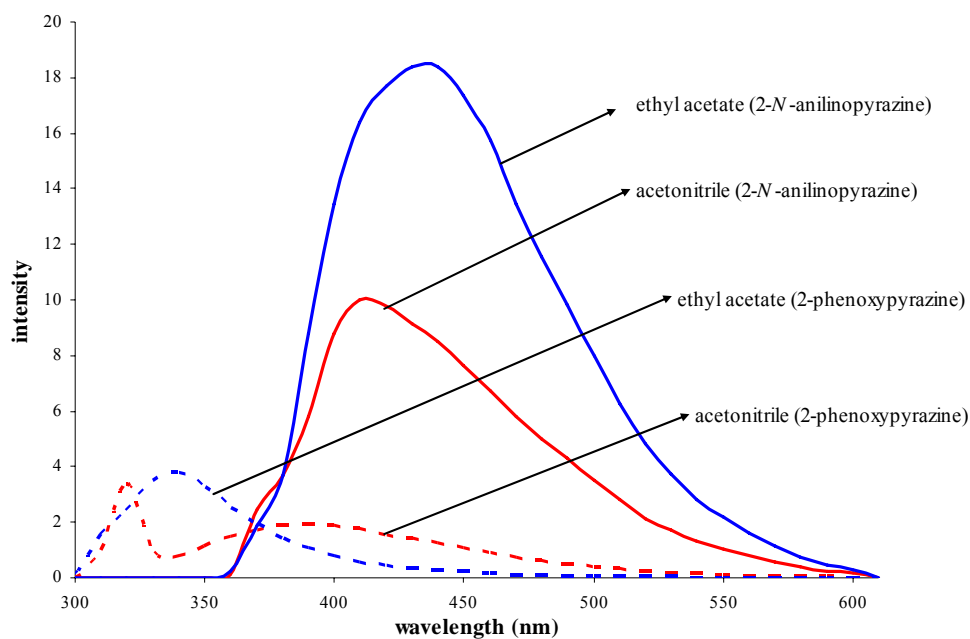


**Figure 3.22: Fluorescence spectra of 2-*N*-anilinoquinoxaline (46) and 2-phenoxyquinoxaline (55) in ethyl acetate and acetonitrile in capped condition**

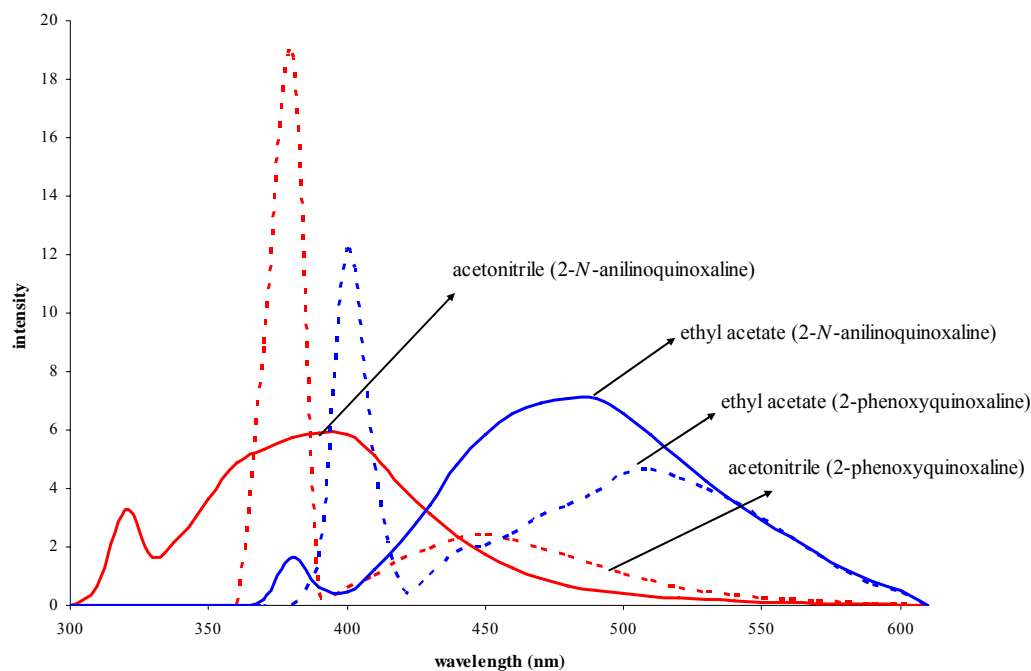


**Figure 3.23: Fluorescence spectra of 2-*N*-anilinoquinoxaline (**62**) and 2-phenoxyquinoxaline (**68**) in ethyl acetate and acetonitrile in capped condition**

Table 3.11 shows that 2-*N*-anilinopyrazine (**46**) has the higher fluorescence intensity than 2-phenoxyprazine (**55**) in various solvents. This can also be seen in Figure 3.22. This observation could be due to the presence of oxygen in the system of (**55**) which is a heavy atom. Oxygen is heavier than nitrogen, as the result this may be associated with a reduction in fluorescence efficiency, which favours the  $n \rightarrow \pi^*$  transition rather than  $\pi \rightarrow \pi^*$  transition. As the result, phosphorescence was favoured and a reduction in fluorescence intensity was observed. The same reason applies to the phenomena observed with 2-phenoxyquinoxaline (**68**), as shown in Figure 3.23. It can be clearly seen that the amino derivatives are more fluorescent than phenoxy derivatives.

The effect of substituents on 2-substituted pyrazine and 2-substituted quinoxaline system were studied with a series of 2-substituted anilinopyrazine and 2-substituted anilinoquinoxaline. Table 3.13 and Table 3.14 show the fluorescence characteristic of compound (46), (50), (51), (62), (66) and (67) in acetonitrile, and Figure 3.24 and Figure 3.25 show the fluorescence spectra of the above compounds.

**Table 3.13: Fluorescence characteristic of compounds (46), (50) and (51) in acetonitrile in  $10^{-4}$  M**

2-Y-pyrazine	Solvent	Excitation wavelength (nm)	Fluorescence wavelength (nm)	Intensity
-N-anilino (46)	Acetonitrile	377	414	10.09
-N-( <i>p</i> -methoxy)anilino (50)	Acetonitrile	458	487	3.74
-N-( <i>p</i> -chloro)anilino (51)	Acetonitrile	358	464	3.23

**Table 3.14: Fluorescence characteristic of compounds (62), (66) and (67) in acetonitrile in  $10^{-4}$  M**

2-Y-quinoxaline	Solvent	Excitation wavelength (nm)	Fluorescence wavelength (nm)	Intensity
-N-anilino (62)	Acetonitrile	314	411	10.69
-N-( <i>p</i> -methoxy)anilino (66)	Acetonitrile	434	472	12.98
-N-( <i>p</i> -chloro)anilino (67)	Acetonitrile	395	498	0.76

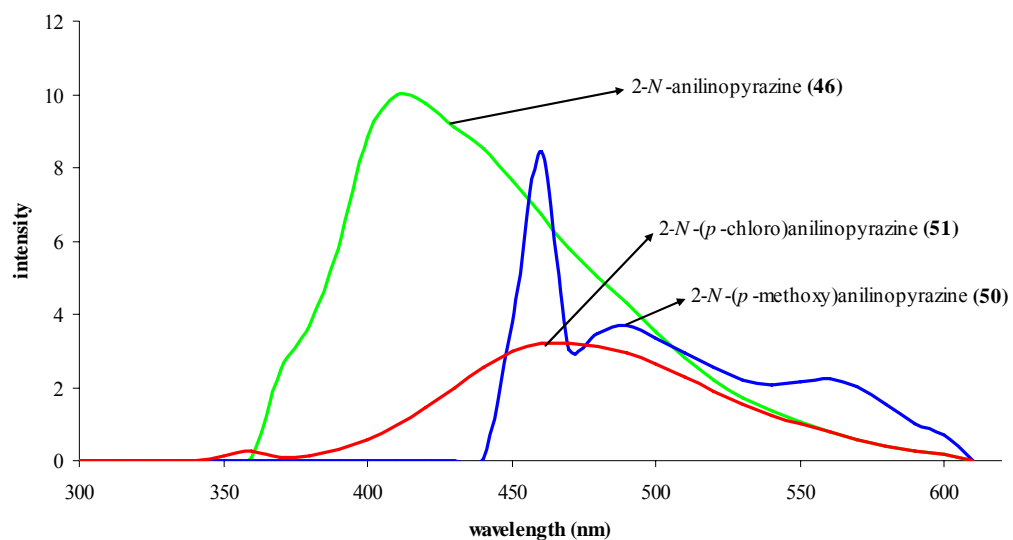


**Figure 3.24: Fluorescence spectra of compounds (46), (51) and (50) in acetonitrile in  $10^{-4}$  M**

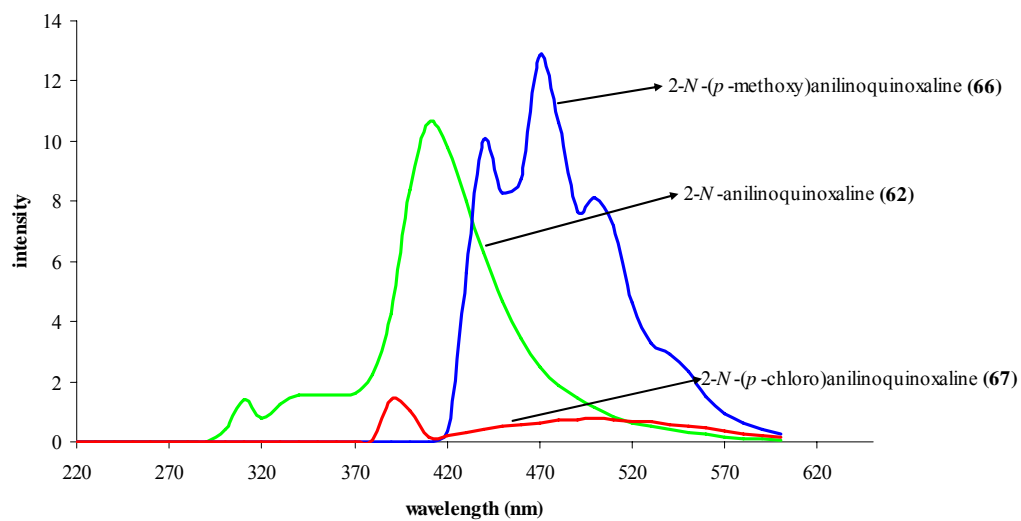


**Figure 3.25: Fluorescence spectra of compounds (62), (66) and (67) in acetonitrile in  $10^{-4}$  M**

It can be seen from Table 3.13 and Table 3.14 that substitution in a conjugated system has profound effect on the fluorescent properties. Some substitutions of the parent nucleus cause a bathchromic shift. The extent of this shift is significantly higher for an electron donating substituent.<sup>124</sup> This can be seen in Figure 3.24, the fluorescent wavelength maxima of 2-*N*-(*p*-methoxy)anilinopyrazine (**50**), 2-*N*-(*p*-chloro)anilinopyrazine (**51**) undergo a shift to a longer wavelength than 2-*N*-anilinopyrazine (**46**), reflecting the delocalisation of the  $\pi$  electrons in the system. Similar observation was also seen in Figure 3.25 for 2-substituted anilinoquinoxaline which is believed to be of the same reason mentioned above.

2-*N*-(*p*-Chloro)anilinopyrazine (**51**) showed the lower fluorescence intensity than 2-*N*-(*p*-methoxy)anilinopyrazine (**50**) as shown in Table 3.13. This low value was attributed to the enhancement of intersystem crossing due to the presence of heavy atom effect of the chlorine in the solvent molecule. This is also probably because chlorine is an electron withdrawing group whereas methoxy is electron donating group. The methoxy group tends to enhance fluorescence due to the electron mobility. The observed fluorescence intensity of 2-*N*-(*p*-chloro)anilinoquinoxaline (**67**) which is less fluoresce than 2-*N*-(*p*-methoxy)anilinoquinoxaline (**66**) is believed to be due to the same reason as in the pyrazine system as discussed earlier.

Stevenson<sup>118</sup> has studied the effects on the absorption spectrum of benzene by substituents. Alkyl substituents on the aromatic ring generally produce a bathchromic displacement in both the absorption and the fluorescence spectrum. Thus, the spectra of toluene are found to be displaced toward the red when compared with those of benzene.

Monosubstituted compounds containing OH, OCH<sub>3</sub>, NH<sub>2</sub>, N(CH<sub>3</sub>)<sub>2</sub>, F and C≡N are fluorescent, while those containing NHCOCH<sub>3</sub>, Cl, Br, I, C=O, NO<sub>2</sub>, SO<sub>3</sub>H and COOH are likely to be weakly or non fluorescent. The presence of bromine, iodine, or heavy metal substituents in either mono or poly-substituted aromatic compounds invariably leads to a reduction in fluorescence by encouraging intersystem crossing from the excited state to the triplet state.

In general, electron donating substituents capable to increase the fluorescence intensity while electron withdrawing substituents capable to decrease it. Nevertheless, some experimental results are contradictive to the theoretical expectations. In a series of 2-substituted anilinopyrazine as shown in Table 3.13, the fluorescence intensity of compound **(50)** was less fluorescent than compound **(46)**. This result is opposite to the known information that fluorescence intensity increases by introducing electron donating substituent. Similar phenomena were observed in a series of 2-substituted anilinopyrazine and 2-substituted anilinoquinoxaline in different solvents. The spectral data of these compounds are as shown in experimental section. These exceptions are probably due to the substituent groups that can interact strongly with the solvent. In other words, for aromatic compounds with different functional groups it is impossible to separate structural from environmental effects on their fluorescence behaviour.

Table 3.15 shows the fluorescence characteristic of compound **(57)**, **(64)**, **(66)**, **(68)** and **(69)** with time in THF, and Figure 3.26 and Figure 3.27 show the fluorescence spectra of compound **(57)** and **(69)** with the measurements were taken immediately, followed by after 20 minutes and 40 minutes respectively.

**Table 3.15: Fluorescence characteristic of selected pyrazine and quinoxaline derivatives in different time in THF**

Compound	Duration (min)	Excitation wavelength (nm)	Fluorescence wavelength (nm)	Intensity
2-( <i>p</i> -methyl) phenoxy pyrazine ( <b>57</b> )	Immediately	310	286	65.53
	20		391	62.77
	40		385	61.93
2- <i>N</i> -( <i>p</i> -methyl) anilinoquinoxaline ( <b>64</b> )	Immediately	411	500	4.92
	20		502	4.89
	40		516	4.74
2- <i>N</i> -( <i>p</i> -methoxy)anilinoquinoxaline ( <b>66</b> )	Immediately	437	471	32.23
	20		473	31.15
	40		472	29.67
2-phenoxyquinoxaline ( <b>68</b> )	Immediately	387	428	6.24
	20		429	4.80
	40		427	4.45
2-( <i>m</i> -methyl) phenoxyquinoxaline ( <b>69</b> )	Immediately	420	516	501.99
	20		516	495.03
	40		515	485.83

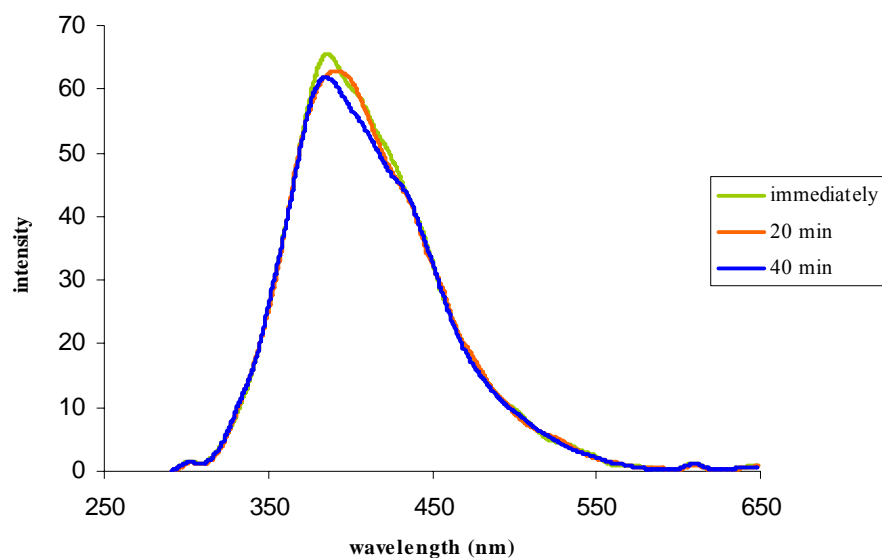


**Figure 3.26: Fluorescence spectra of 2-(*p*-methyl)phenoxy pyrazine (**57**) in different time in THF ( $5.3703 \times 10^{-4}$  M)**

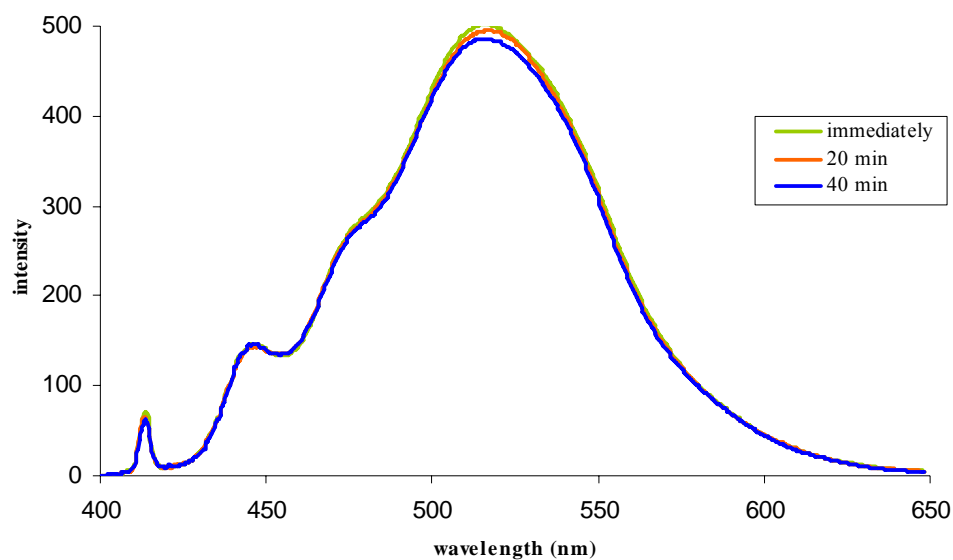


**Figure 3.27: Fluorescence spectra of 2-(*m*-methyl)phenoxyquinoxaline (69) in different time in THF ( $4.2324 \times 10^{-4}$  M)**

The study on the effect of oxygen or air and delayed fluorescence on fluorescence characteristics of compounds studied were carried out by measuring the fluorescence of respective compound in capped condition with time. The fluorescence of 2-(*p*-methyl)phenoxy pyrazine (57) and 2-(*m*-methyl)phenoxyquinoxaline (69) showed decrease in intensity with time as shown in Figure 3.26 and Figure 3.27. It can also be seen from Figure 3.26 and Figure 3.27 that, no delayed fluorescence was recorded.

A possible explanation for this phenomenon is the quenching effect of oxygen. Oxygen which has an unusually large diffusion coefficient may entered the solution. As the solution was allowed to stand for 20 minutes and 40 minutes respectively, the oxygen quenched the fluorescence peak as the result a decrease in fluorescence intensity was observed. It is suggested that the quenching effect was due to the formation of a complex between the compound studied and oxygen. However, more work need to be carried out before a concrete conclusion can be made.

However, in the case of 2-*N*-anilinoquinoxaline (**62**), an increase in intensity was observed with time as shown in Table 3.16. This increased of fluorescence intensity may be due to the delayed fluorescence phenomena. Delayed fluorescence is spectrally similar to the ordinary fluorescence but has a considerably longer lifetime. This results from thermal excitation of the triplet and reoccupation of the first excited singlet followed by fluorescence. This type of fluorescence has been found for many molecules including phenanthrene, anthracene and pyrene.<sup>125</sup> The fluorescence spectra of 2-*N*-anilinoquinoxaline (**62**) as shown in Figure 3.28.

**Table 3.16: Fluorescence characteristic of 2-*N*-anilinoquinoxaline (**62**) in different time in THF ( $4.5195 \times 10^{-4}$  M)**

Solvent	Duration (min)	Excitation wavelength (nm)	Fluorescence wavelength (nm)	Intensity
THF	Immediately	380	472	20.83
	20		473	23.98
	40		472	25.29

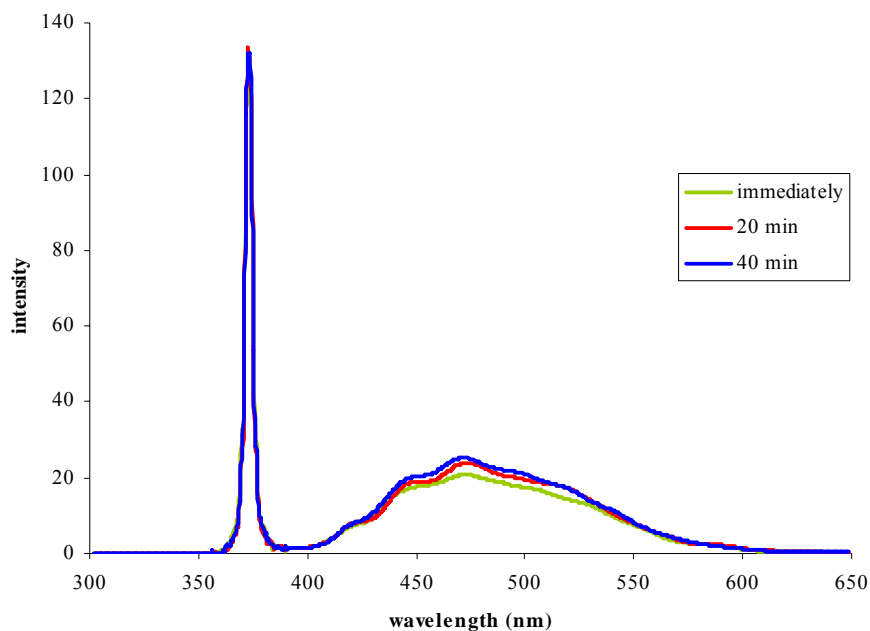


**Figure 3.28: Fluorescence spectra of 2-*N*-anilinoquinoxaline (**62**) in different time in THF ( $4.5195 \times 10^{-4}$  M)**

Table 3.17, Table 3.18 and Table 3.19 show the fluorescence characteristic of 2-*N*-piperidinopyrazine (**37**), 2-*N*-(*m*-methyl)piperidinopyrazine (**38**) and 2-*N*-(*p*-methyl)piperidinopyrazine (**39**) with respect to concentrations of  $10^{-4}$ M,  $10^{-5}$ M, and  $10^{-6}$  M in various solvents respectively. Figure 3.29 to Figure 3.31 show their fluorescence spectra.

**Table 3.17: Fluorescence characteristic of 2-*N*-piperidinopyrazine (**37**) in different concentrations**

Solvent	Excitation wavelength (nm)			Fluorescence wavelength (nm)			Intensity		
	$10^{-6}$ M	$10^{-5}$ M	$10^{-4}$ M	$10^{-6}$ M	$10^{-5}$ M	$10^{-4}$ M	$10^{-6}$ M	$10^{-5}$ M	$10^{-4}$ M
THF	345	348	369	403	402	401	62.27	382.70	560.50
CH <sub>3</sub> CN	348	348	371	411	415	419	51.64	262.40	460.60
EtOAc	344	345	362	404	407	408	26.30	159.80	441.70
EtOH	349	350	373	422	432	431	4.18	25.67	51.31

Concentration =  $6.1270 \times 10^x$  M, where  $10^x$  M =  $10^{-6}$  M,  $10^{-5}$  M,  $10^{-4}$  M

**Table 3.18: Fluorescence characteristic of 2-*N*-(*m*-methyl)piperidinopyrazine (**38**) in different concentrations**

Solvent	Excitation wavelength (nm)			Fluorescence wavelength (nm)			Intensity		
	$10^{-6}$ M	$10^{-5}$ M	$10^{-4}$ M	$10^{-6}$ M	$10^{-5}$ M	$10^{-4}$ M	$10^{-6}$ M	$10^{-5}$ M	$10^{-4}$ M
THF	347	347	362	402	404	401	27.42	235.30	505.40
CH <sub>3</sub> CN	347	348	354	414	414	414	11.31	84.34	364.80
EtOAc	345	346	356	401	404	405	15.32	119.10	398.10
EtOH	348	349	363	424	424	432	3.375	23.51	70.32

Concentration =  $5.5785 \times 10^x$  M, where  $10^x$  M =  $10^{-6}$  M,  $10^{-5}$  M,  $10^{-4}$  M

**Table 3.19: Fluorescence characteristic of 2-*N*-(*p*-methyl)piperidinopyrazine (39) in different concentrations**

Solvent	Excitation wavelength (nm)			Fluorescence wavelength (nm)			Intensity		
	10 <sup>-6</sup> M	10 <sup>-5</sup> M	10 <sup>-4</sup> M	10 <sup>-6</sup> M	10 <sup>-5</sup> M	10 <sup>-4</sup> M	10 <sup>-6</sup> M	10 <sup>-5</sup> M	10 <sup>-4</sup> M
THF	345	347	360	402	400	403	29.62	208.00	518.50
CH <sub>3</sub> CN	347	348	360	411	415	415	17.80	130.30	399.60
EtOAc	343	345	358	404	404	404	21.88	149.60	399.10
EtOH	348	350	363	425	430	427	2.56	15.31	45.86

Concentration = 5.5785 x 10<sup>x</sup> M, where 10<sup>x</sup> M = 10<sup>-6</sup> M, 10<sup>-5</sup> M, 10<sup>-4</sup> M

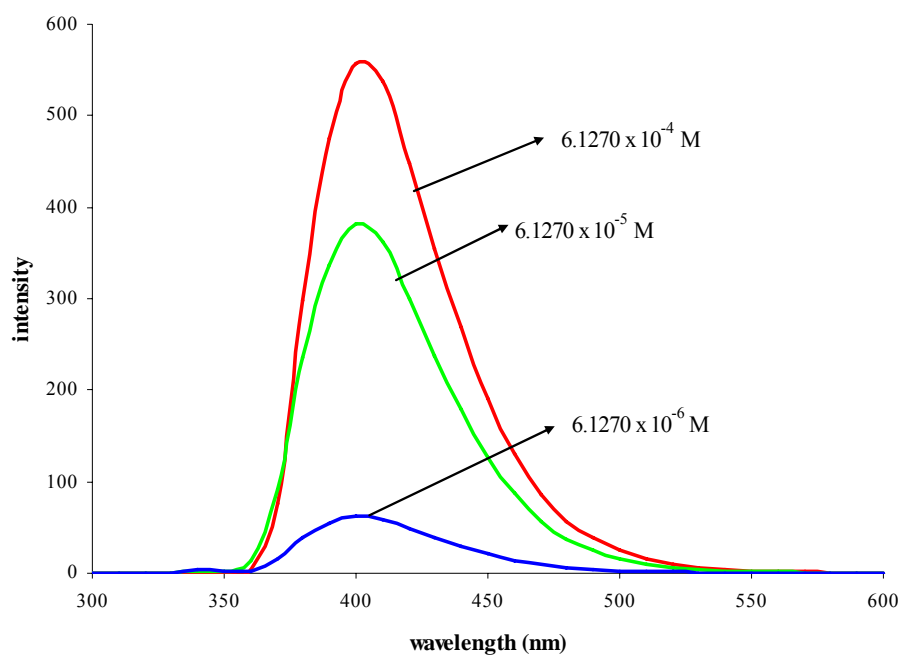


**Figure 3.29: Fluorescence spectra of 2-*N*-piperidinopyrazine (37) in different concentrations in THF**

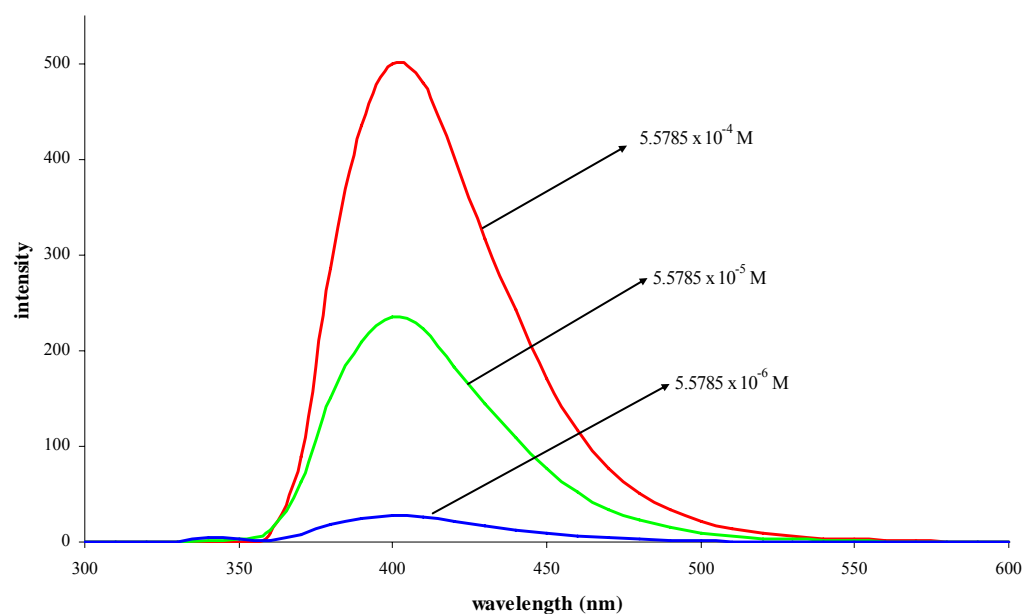


**Figure 3.30: Fluorescence spectra of 2-*N*-(*m*-methyl)piperidinopyrazine (38) in different concentrations in THF**

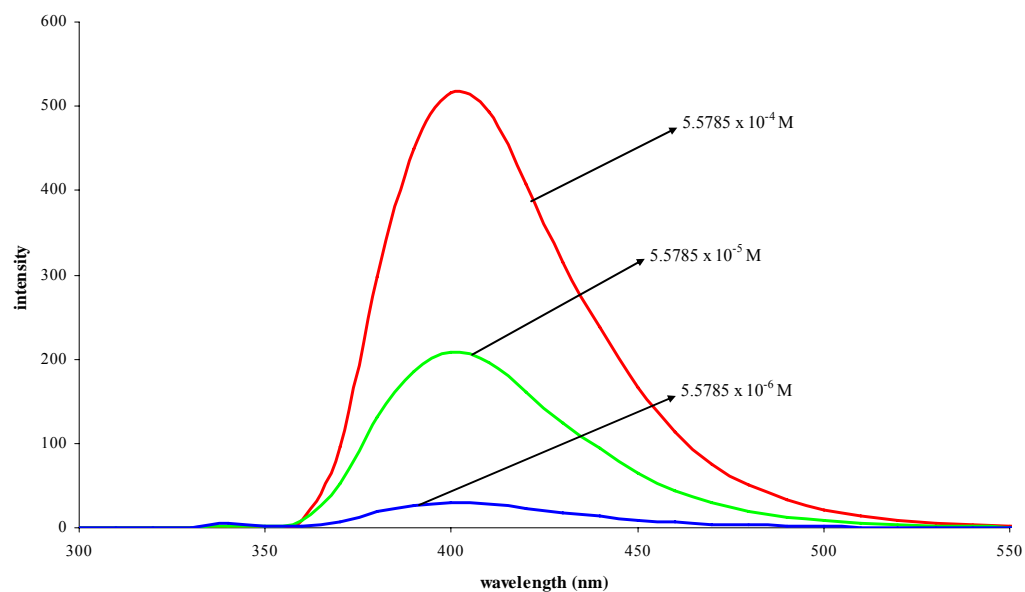


**Figure 3.31: Fluorescence spectra of 2-*N*-(*p*-methyl)piperidinopyrazine (39) in different concentrations in THF**

It was found that the fluorescence intensity increases linearly with increasing concentration at relatively low concentrations. It can be seen from Table 3.17, Table 3.18 and Table 3.19 that higher concentration tends to increase the fluorescence intensity for compound (37), (38) and (39). It has been reported that at higher concentrations, the fluorescence intensity may reach a limiting value and usually result in concentration quenching which decrease with further increases in concentration and is often accompanied by wavelength shifts.<sup>126</sup>

It is also known that in the limit of high absorber concentration, the linearity between absorbance and concentration breaks down. In very concentrated solutions, the absorbance may become infinite because all of the exciting light will be absorbed before it can completely penetrate the sample cell. On the other hand, the high concentration of sample results in a variety of molecular interactions, such as collisional quenching and energy transfer, which can distort the fluorescence spectrum.<sup>126</sup> In this study, those observations were not seen because the concentrations used did not reach the limit value.

Lavorel<sup>127</sup> has demonstrated that at high concentrations of fluorescein, thionine and chlorophyll dimerisation occurs. The absorption spectra of these dimers have differ from the parent compounds and in these instances, the dimers have different spectral properties. It is apparent that when more than one molecular absorbing species is present in a solution, fluorescence efficiency will not be constant over the entire spectrum.

Apart from concentration, the change of pH also affects the fluorescence intensity of the heterocyclic compounds studied. A detailed study covering five different pH values is made for a better understanding of the fluorescence characteristic of selected 2-substituted pyrazines and 2-substituted quinoxalines. Selected data on fluorescence maxima and intensities for these compounds are as summarised in Table 3.20 and Table 3.21, while their fluorescence spectra in ethanol are shown in Figure 3.32 and Figure 3.33.

**Table 3.20: Fluorescence characteristic of 2-*N*-piperidinopyrazine (37) and 2-*N*-anilinopyrazine (46) with variation of pH in ethanol**

2-Y-pyrazine	Conditions	pH	Excitation wavelength (nm)	Fluorescence wavelength (nm)	Intensity
<i>N</i> -piperidino (37)	acid	2	359	439	106.20
		3	365	433	269.70
	neutral	7	373	432	287.50
	base	11	368	431	277.90
		12	368	433	259.10
<i>N</i> -anilino (46)	acid	2	382	433	3.79
		3	393	492	6.49
	neutral	7	399	493	12.25
	base	11	395	491	7.71
		12	393	490	7.48

**Table 3.21: Fluorescence characteristic of 2-*N*-piperidinoquinoxaline (59) and 2-*N*-anilinoquinoxaline (62) with variation of pH in ethanol**

2-Y-quinoxaline	Conditions	pH	Excitation wavelength (nm)	Fluorescence wavelength (nm)	Intensity
<i>N</i> -piperidino (59)	acid	2	409	455	143.00
		3	410	455	157.80
	neutral	7	418	455	159.40
	base	11	410	455	154.20
		12	409	455	158.60
<i>N</i> -anilino (62)	acid	2	336	454	2.10
		3	419	483	2.36
	neutral	7	313	482	5.17
	base	11	422	483	2.60
		12	418	483	2.62

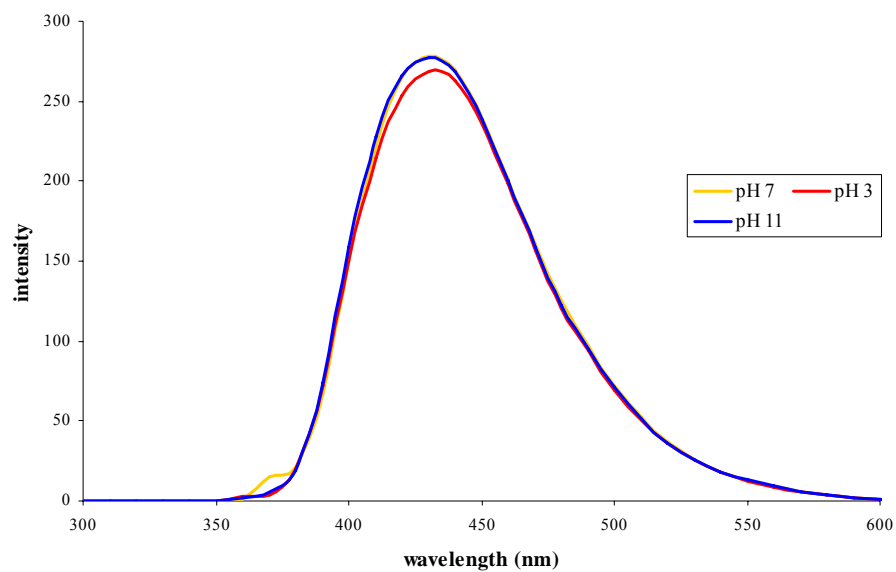


**Figure 3.32: Fluorescence spectra of 2-*N*-piperidinopyrazine (37) with variation of pH**

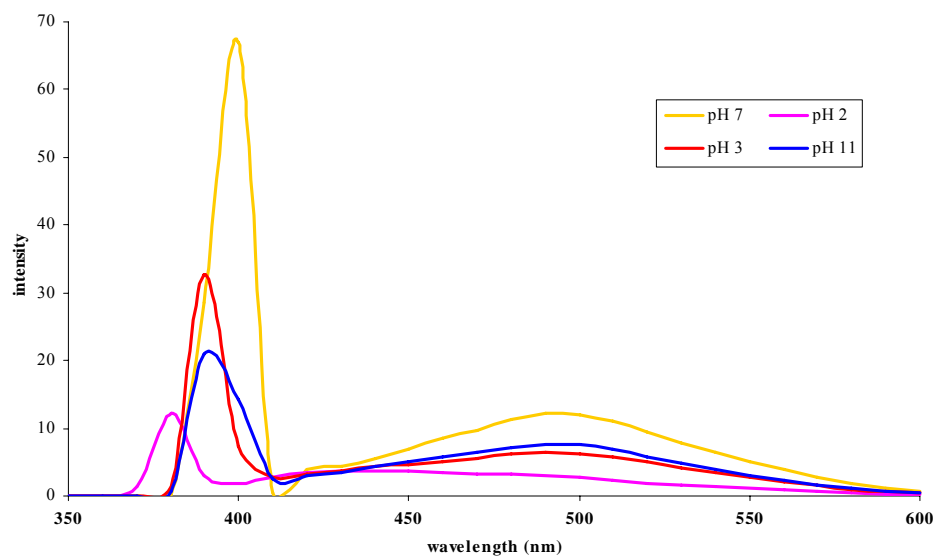


**Figure 3.33: Fluorescence spectra of 2-*N*-anilinopyrazine (46) with variation of pH**

The fluorescence spectra for 2-*N*-piperidinopyrazine (**37**), 2-*N*-anilinopyrazine (**46**), 2-*N*-piperidinoquinoxaline (**59**) and 2-*N*-anilinoquinoxaline (**62**) were measured in ethanol under neutral, acidic (0.1 M HCl) and basic (0.1 M NaOH) conditions. From Table 3.20 and Table 3.21, it is noticeable that in all cases, all of these compounds showed highest fluorescence intensity under neutral conditions. On the other hand, under acidic and basic conditions, the intensity of fluorescence of these compounds was lower. This is due to the fluorescence solvatochromism, which is strong under neutral conditions and relatively weak in acid or base which is in an agreement with the work done previously.<sup>128</sup>

Table 3.20 and Table 3.21 also show that the fluorescence intensity gradually increases with the increase of pH. The low fluorescence intensity observed in acidic medium is probably due to protonation of the compound. The hydrogen atom abstraction from protonated form yielded the lowest intensity which involves the transferring of the proton to the ring nitrogen as shown in Figure 3.34 and Figure 3.35. As the result, therefore the fluorescence is completely quenched. The corresponding electrons phenomena results in a non-conjugated system which results in non-fluorescent compounds. This phenomena was proved by Weisstuch and Testa<sup>121</sup> and similar observation on purinyl ring was reported by Haroutounian and Katzenellenbogen.<sup>128</sup>

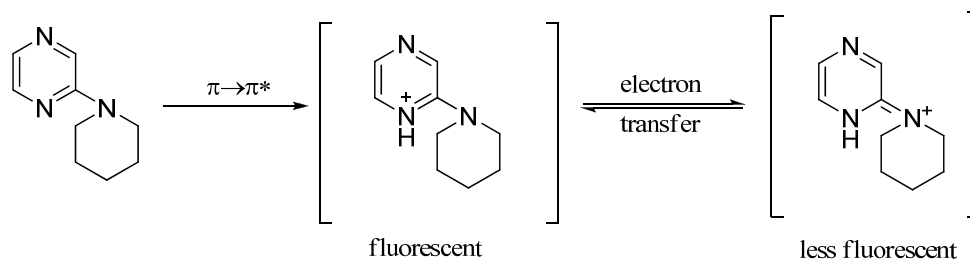


**Figure 3.34: The proton transfer to the ring nitrogen of 2-*N*-piperidinopyrazine (**37**)**

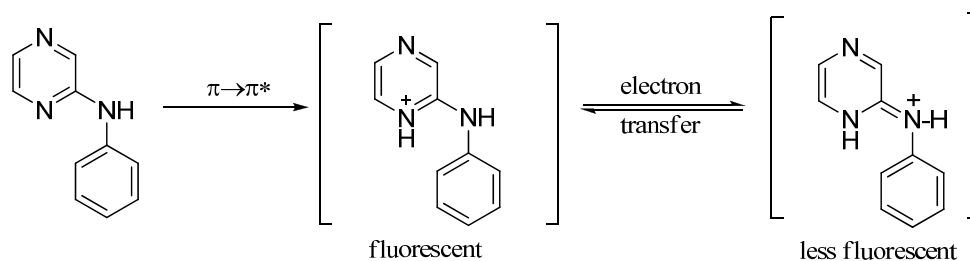


**Figure 3.35: The proton transfer to the ring nitrogen of 2-*N*-anilinopyrazine (46)**

Studies show that, compounds (37), (46), (59) and (62) fluoresced at higher intensities in neutral and basic media. However, upon acidification (pH 3), these compounds undergo reductions in its maximum intensity due to the reasons explained earlier. A further increase in acidity (pH 2), resulted in a further decrease in the fluorescence intensity of compounds.